ORIGINAL ARTICLE

Revealing the diversity of the green *Eulalia* (Annelida, Phyllodocidae) species complex along the European coast, with description of three new species

Marcos A. L. Teixeira[1,2] · **Pedro E. Vieira**[1,2] · **David Fenwick**[3] · **Joachim Langeneck**[4] · **Fredrik Pleijel**[5] · **Bruno R. Sampieri**[6] · **José Carlos Hernández**[7] · **Ascensão Ravara**[8] · **Filipe O. Costa**[1,2] · **Arne Nygren**[5]

Abstract

The green phyllodocids *Eulalia clavigera* and *E. viridis* are a known European pseudo-cryptic complex, but questions about its distribution and evidence of additional lineages in previous studies call for an investigation of the real diversity within the complex. We analyze DNA sequences (mtCOI-5P, ITS, and 28S rRNA) of different populations of *E. clavigera* from intertidal and subtidal marine waters along the North East Atlantic, Mediterranean Sea, the Azores and Webbnesia (Madeira, Savage islands and Canaries), and populations of *E. viridis* from the Scandinavia. This provided compelling evidence for the existence of six additional divergent evolutionary lineages, three of the most abundant being described here as new species: *Eulalia feliciae* sp. nov., intertidal and unique to the Western Mediterranean, *Eulalia madeirensis* sp. nov., subtidal and unique to the Madeira Island (Portugal), and *Eulalia xanthomucosa* sp. nov., mostly subtidal and occurring in the British Isles and southern France. Complementary morphometric analyses showed that *E. feliciae* sp. nov. and *E. madeirensis* sp. nov. formed two independent morphometric clusters, while *E. xanthomucosa* sp. nov. often overlapped with *E. clavigera* sensu stricto *(s. s.)*, although being unique in showing a yellow coloration and parapodial cirri on median segments larger in relation to its body size. Recent biotechnological findings based on "*E. clavigera*" specimens highlight the importance of formally describing cryptic complexes, since each lineage chemistry might be unique and may have a range of distinct effects and applications.

Introduction

Biodiversity may vary at genetic, species, and ecosystem levels, with the true animal diversity being appraised in-deep by using molecular tools to detect cryptic or pseudo-cryptic species. Pseudo-cryptic complexes constitute a substantial fraction of biodiversity and appear to be frequent among marine benthic invertebrates (Miglietta et al., 2011; Nygren, 2014) in well-known taxa and areas (e.g., Bleidorn et al., 2006; Carr et al., 2011; Grosse et al., 2021; Jolly et al., 2006;

✉ Marcos A. L. Teixeira
mark-us_teixeira@hotmail.com

1 Centre of Molecular and Environmental Biology (CBMA), Department of Biology, University of Minho, Campus de Gualtar, Braga 4710-057, Portugal

2 Institute of Science and Innovation for Bio-Sustainability (IB-S), University of Minho, Campus de Gualtar, Braga 4710-057, Portugal

3 Myrtles Court, Saltash, Cornwall, UK

4 Consorzio Nazionale Interuniversitario per Le Scienze del Mare (CoNISMa), U.L.R. Di Lecce, via provinciale Lecce-Monteroni, Campus Ecotekne, 73100 Lecce, Italy

5 Institutionen for marina vetenskaper, Göteborgs Universitet, Strömstad, Tjärnö, Sweden

6 Museu de Zoologia da Universidade Estadual de Campinas–IB/UNICAMP, Instituto de Biologia, Rua Charles Darwin, Bloco N, Cidade Universitária, Campinas, SP, Brasil

7 Biología Animal, Edafología Y Geología, Universidad de La Laguna, Tenerife, Spain

8 Centre for Environmental and Marine Studies (CESAM), Department of Biology, University of Aveiro, Campus de Santiago, Aveiro 3810-193, Portugal

GfBS

Leite et al., 2020; Lobo et al., 2017). Despite the increasing evidence of cryptic species occurrence, the lack of formal taxonomic description (Fernandez-Triana, 2022) hinders accurate estimates of their contribution to biodiversity (Delić et al., 2017; Fišer et al., 2018; Hutchings & Kupriyanova, 2018); therefore, limiting our understanding of their evolutionary and ecological significance, as well as their recognition in large scale biomonitoring programs using high throughput sequence technologies.

The homogeneously green phyllodocid, *Eulalia viridis* (Linnaeus, 1767), has been reported from throughout the northern hemisphere (Eibye-Jacobsen, 1991, 1993). It is common in intertidal and subtidal coastal areas and marinas, down to 50 m depth (Ushakov, 1972), usually living on rocky reefs in crevices, among algae, mussel beds, *Balanus* spp. blocks, *Dendropoma* reefs, *Posidonia oceanica* (Linnaeus) Delile, 1813 meadows, and coralligenous formations (Bonse et al., 1996; Viéitez et al., 2004; Çinar, 2005). However, in Mediterranean *Sabellaria alveolata* (Linnaeus, 1767) reefs, it is replaced by *Eulalia ornata* Saint-Joseph 1888, faint yellow but sometimes greenish species morphologically similar to *E. viridis*, except for the pigmentation pattern (Schimmenti et al., 2016).

Based on isoelectric focusing and morphological data, a correlation between exclusive isoenzymes and protein patterns, the morphology and size of the mid-body dorsal cirri, and the size of the proboscideal papillae allowed to discriminate between two distinct groups of *Eulalia* populations (Bonse et al., 1996). The morphotype from the North Sea and Scandinavian coasts, showing smaller papillae and slender dorsal cirri, corresponded to *E. viridis*, while that from France and England showing larger papillae and significantly thicker dorsal cirri was attributed to *Eulalia clavigera* (Audouin & Milne-Edwards, 1833), hitherto synonymized with *E. viridis*. The reproductive biology of phyllodocids is poorly known, and these two species are not an exception. They have planktonic larval stages and reproduce once a year (Meyer, 1938), but Northern Europe populations also differ locally in reproduction time, with reproductive cycle starting four to six weeks earlier in Sweden than in England and France (Olive, 1975; Pleijel, 1993). The green *Eulalia sp.* is a predator feeding mostly on mussels and barnacles (Rodrigo et al., 2015), with occasional scavenger habits also being observed (Morton, 2011). Molecular studies based on the mitochondrial cytochrome c oxidase subunit I (COI) also allowed distinguishing two populations of *Eulalia viridis* from Kandalaksha Bay (Russia) and Portugal, which showed more than 20% Kimura's two parameter (K2P) genetic divergence (Hardy et al., 2011; Lobo et al., 2016). Their highly similar morphology and the large number of discriminating genetic markers certainly imply the existence of a pseudo-cryptic species complex. A South-Western

population of *E. clavigera* from Patagonia did not show any genetic differentiation toward the North-Eastern Atlantic specimens, supporting a non-native origin of the Patagonian population (Langeneck et al., 2019). However, Mediterranean specimens examined by Langeneck et al. (2019) represented a distinct lineage compared to the Patagonia/North East Atlantic clade.

Given the high number of species complexes among phyllodocid genera, such as *Notophyllum* (Nygren et al., 2010) or *Eumida* (Nygren & Pleijel, 2011; Teixeira et al., 2022), and among other polychaete families (Grosse et al., 2021; Lobo et al., 2016; Sampieri et al., 2021), the actual diversity and distribution of European species of the *Eulalia viridis/clavigera* species group is questioned. In this study, we use a combined multi-locus and morphometric approach to compare the European populations of *E. clavigera*, from the United Kingdom to Portugal, the Azores and Webbnesia (Madeira, Savage islands and Canaries), and the Western and Eastern Mediterranean Sea, as well as molecular data for populations of *E. viridis* from the Scandinavia to investigate the possible occurrence of additional diagnosable species within the *Eulalia viridis/clavigera* complex.

Methods

Taxon sampling and molecular data retrieval

We sampled a total of 131 specimens of *Eulalia*, belonging to the *Eulalia clavigera/viridis* complex, three of *Eulalia aurea* Gravier, 1896 and one of *Phyllodoce* Lamarck, and 1818 distributed along the European coasts, including the Azores and Webbnesia (Fig. 1). Worms were collected at low tide in rocky beaches among algae and mussels in marinas or subtidal areas up to 34 meters in depth and fixed in 96% ethanol. Samples were harvested in continental Portugal (Canto Marinho, Leixoes, Aveiro, and Nazaré), Santa Maria (Azores) and Madeira islands, Spain (La Coruña and the islands of Tenerife, Gran Canaria, and La Palma), France (Roscoff, Morgat, Banyuls, and Corsica), Great Britain (Plymouth and Cornwall), Norway (Espevær , Grimstad, Bergen, Trondheim, and Finmark), Sweden (Koster), Italy (Livorno, Ischia island and Taranto), and Croatia (Istria) (Table 1, Table S1).

We sequenced a partial segment of COI 5' end (mtCOI-5P) from 119 specimens and a representative number per location for the ITS-regions (i.e., ITS1, 5.8S rRNA, and ITS2) and 28S rRNA (Table 2). MtCOI-5P sequences belonging to *Eulalia cf. clavigera* from Capraia Island and port of Stintino, Italy (Langeneck et al., 2019), were mined from GenBank for comparison purposes. *Eulalia aurea* and *Phyllodoce* sp. were used as outgroups. DNA was extracted,

Fig. 1 Sampling sites. Abbreviations as in Table 1

amplified, sequenced, and assembled as described in Nygren et al. (2010) or Lobo et al. (2016), depending of the lab and materials available, from a few parapodia or a small portion of the posterior end of the specimens. Morphological and molecular vouchers are deposited in the Research Collection of Marine Invertebrates of the Department of Biology of the University of Aveiro (CoBI-DBUA), in the French Muséum national d'Histoire naturelle (MNHN; specimens MNHN-IA-2021-654 and MNHN-IA-2021-655), Scripps Oceanographic Institution (SIO; French Mediterranean specimen BI-2014/15-077), National Museum of Science and Natural History (MUHNAC, Portugal; specimen MB29-000385 from the Savage islands) and in Arne Nygren's private collection (ANPC; specimens MTE040-20, MTE042-20, MTE052-20, MTE053-20, MTE054-20, MTE055-20, MTE057-20, MTE079-20, MTE080-20, MTE081-20, and MTE088-20) using the Barcode Of Life Data (BOLD) Process ID ("MTE", http://v4.boldsystems.org/) for Arne Nygren's specimens.

The full dataset and its metadata can be accessed at BOLD Systems under the project "*Eulalia* Species Complex (DS-MTE)" (DOI: https://doi.org/10.5883/DS-MTEC), except for the four COI sequences from Langeneck et al. (2019). GenBank accession numbers: OP898309-OP898427 (mtCOI-5P), OP897856-OP897897 (ITS region), and OP897898-OP897939 (28S) (Table S1).

Phylogeny and genetic distances

Maximum likelihood (ML) and Bayesian inference (BI) were used for the phylogenetic analyses. The nuclear markers (ITS-regions and 28S) and mtCOI-5P locus were aligned with MAFFT online (https://mafft.cbrc.jp/alignment/server/, Katoh & Standley, 2013) and concatenated with MEGA 10.0.05 (Kumar et al., 2018). Highly variable regions, extensive gaps, and poorly aligned positions (mainly present in the ITS-regions) were eliminated using Gblocks 0.91b (http://phylogeny.lirmm.fr/phylo_cgi/one_task.cgi?task_type=gblocks; Castresana, 2000), allowing all options for a less stringent selection and not allowing many contiguous non-conserved positions, so that it becomes more

Table 1 Number of specimens (*n*), the institution responsible for storing the vouchers, sampling areas and the respective abbreviations (code)

Code	Region	Location	n	Coordinates		Storing institution
				Latitude	Longitude	
PTA	South	Portugal, Aveiro	6	40°33′32.4″N	8°46′19.2″W	CoBI-DBUA
PTL	European Atlantic Shelf, Atlantic Ocean	Portugal, Marina of Leixões	1	41°10′58.8″N	8°42′18.0″W	
PTC		Portugal, Canto Marinho	10	41°44′13.2″N	8°52′33.6″W	
PTN		Portugal, Nazaré	3	39°36′13.0″N	9°04′44.0″W	
SPC		Spain, La Coruña	5	43°30′07.2″N	8°09′32.4″W	
FRM		France, Morgat	2	48°13′20.3″N	4°29′42.5″W	
FRR	Northeast Atlantic	France, Roscoff	8	48°43′33.6″N	3°58′40.8″W	
GBP		Great Britain, Plymouth	12	50°21′25.2″N	4°07′40.8″W	
GBC		Great Britain, Cornwall	7	50°06′10.8″N	5°32′49.2″W	
SK	Scandinavia, Skagerrak	Sweden, Koster	3	58°52′30.0″N	11°06′14.4″E	
NOE		Norway, Grimstad	3	58°23′09.6″N	8°44′45.6″E	
NOG	Scandinavia, North Sea	Norway, Espever	1	59°34′15.6″N	5°07′51.6″E	
NOB		Norway, Bergen	3	60°14′13.2″N	5°12′03.6″E	
NOT	Scandinavia, Barents Sea	Norway, Finmark	2	70°37′30.0″N	30°30′50.4″E	
NOF	Scandinavia, Norway Sea	Norway, Trondheim	2	63°29′13.2″N	10°22′26.4″E	ANPC (1); CoBI-DBUA (1)
FRBA	Western Mediterranean Sea	France, Banyuls	14	42°28′48.0″N	3°08′06.0″E	SIO (1); CoBI-DBUA (10); ANPC (3)
FRC		France, Corsica	2	41°26′49.2″N	8°54′00.0″E	MNHN
ITL		Italy, Livorno	3	43°32′24.0″N	10°18′00.0″E	CoBI-DBUA
ITI		Italy, Ischia island	2	40°44′42.0″N	13°58′40.8″E	ANPC
ITT	Eastern Mediterranean Sea	Italy, Taranto	1	40°25′33.6″N	17°13′33.6″E	CoBI-DBUA
CI		Croatia, Istria	1	45°04′26.4″N	13°36′39.6″E	
AM	Azorean ecoregion, Atlantic Ocean	Azores, Santa Maria	2	36°57′03.6″N	25°01′04.8″W	CoBI-DBUA (6), ANPC (2)
MF	Webbnesia, Atlantic Ocean	Madeira, Funchal	8	32°38′09.6″N	16°55′51.6″W	CoBI-DBUA (1), ANPC (3)
MP		Madeira, Porto Moniz	4	32°51′38.6″N	17°09′06.3″W	
TE		Canary islands, Tenerife	11	28°34′15.6″N	16°20′02.4″W	
GC		Canary islands, Gran Canaria	5	27°59′06.0″N	15°22′33.6″W	
LP		Canary islands, La Palma	10	28°48′18.0″N	17°45′43.2″W	
SI		Savage islands	1	30°08′23.9″N	15°51′57.6″W	MUHNAC

Table 2 Primers and PCR conditions

Marker	Primer	Fragment	Direction (5′-3′)	PCR thermal cycling conditions	Reference
COI	PolyLCO	658bp	(F) GAYTATWTTCAACAAATCATA AAGATATTGG	(1) 94 °C (1 min); (2) 5 cycles: 94 °C (40 s), 45 °C (40 s), 72 °C (1 min); (3) 35 cycles: 94 °C (40 s), 51 °C (40 s), 72 °C (1 min); (4) 72 °C (5 min).	Carr et al. (2011)
	PolyHCO		(R) TAMACTTCWGGGTGACCAAAR AATCA		
	LCO1490		(F) GGTCAACAAATCATAAAGATA TTGG	(1) 94 °C (1 min); (2) 5 cycles: 94 °C (30 s), 45 °C (1 min 30 s), 72 °C (1 min); (3) 35 cycles: 94 °C (30 s), 51 °C (1 min 30 s), 72 °C (1 min); (4) 72 °C (5 min).	Folmer et al. (1994)
	HCO2198		(R) TAAACTTCAGGGTGACCAAAA AATCA		
	COI-E		(R) TATACTTCTGGGTGTCCGAAG AATCA		Bely et al. (2004)
ITS1	ITS18Sfa	c.775bp	(F) GAGGAAGTAAAAGTCGTAACA	(1) 96 °C (4 min); (2) 45 cycles: 94 °C (30 s), 62 °C (30 s), 72 °C (1 min); (3) 72 °C (8 min).	Barfuss (2012)
	ITS5.8Sra		(R) GTTCAATGTGTCCTGCAATTC		
ITS2	ITS5.8SF	c.375bp	(F) ATGCTTAAATTCAGCGGGT		Nygren et al. (2009)
	ITS28SR		(R) GAATTGCAGGACACATTGAAC		
28S	28sC1	c.765bp	(F) ACCCGCTGAATTTAAGCAT		Hassouna et al. (1984)
	28s-D2		(R) TCCGTGTTTCAAGACGG		

suitable for a phylogenetic analyses. We used MrBayes 3.1.2 (Ronquist & Huelsenbeck, 2003) for Bayesian analysis. Best-fit models were selected using the Akaike Information Criterion (AIC) in the JModeltest software (Darriba et al., 2012; Guindon & Gascuel, 2003). For mtCOI-5P, we applied the Hasegawa-Kishino-Yano gamma distributed rates across sites (HKY + G) for the first two positions and the HKY model with equal rates across sites for the third position. Regarding the concatenated ITS with 28S, we applied the General Time Reversible (GTR) model with equal rates across sites. The number of generations was set to 10^7, and the sample frequency every 500 generations. Twenty-five percent of the samples were discarded as burn-in (burnin-frac = 0.25). The resulting tree files were checked for convergence in the effective sampling sizes (ESSs > 200) with Tracer 1.6 software (Rambaut et al., 2018) and then analyzed in Figtree 1.4.3 (https://tree.bio.ed.ac.uk/software/figtree/). The final concatenated tree was edited with the software Inkscape 0.92.3 (https://www.inkscape.org). ML phylogenies were performed in MEGA 10.0.05 with 1000 bootstrap runs with the GTR model and equal rates across sites for the concatenated dataset. Only the BI tree is shown in Results, including the ML support if topologies are similar. The alignments (FASTA and NEXUS format) for each individual marker and the concatenated ones are all publicly available at Figshare (DOI: https://doi.org/10.6084/m9.figshare.21657416).
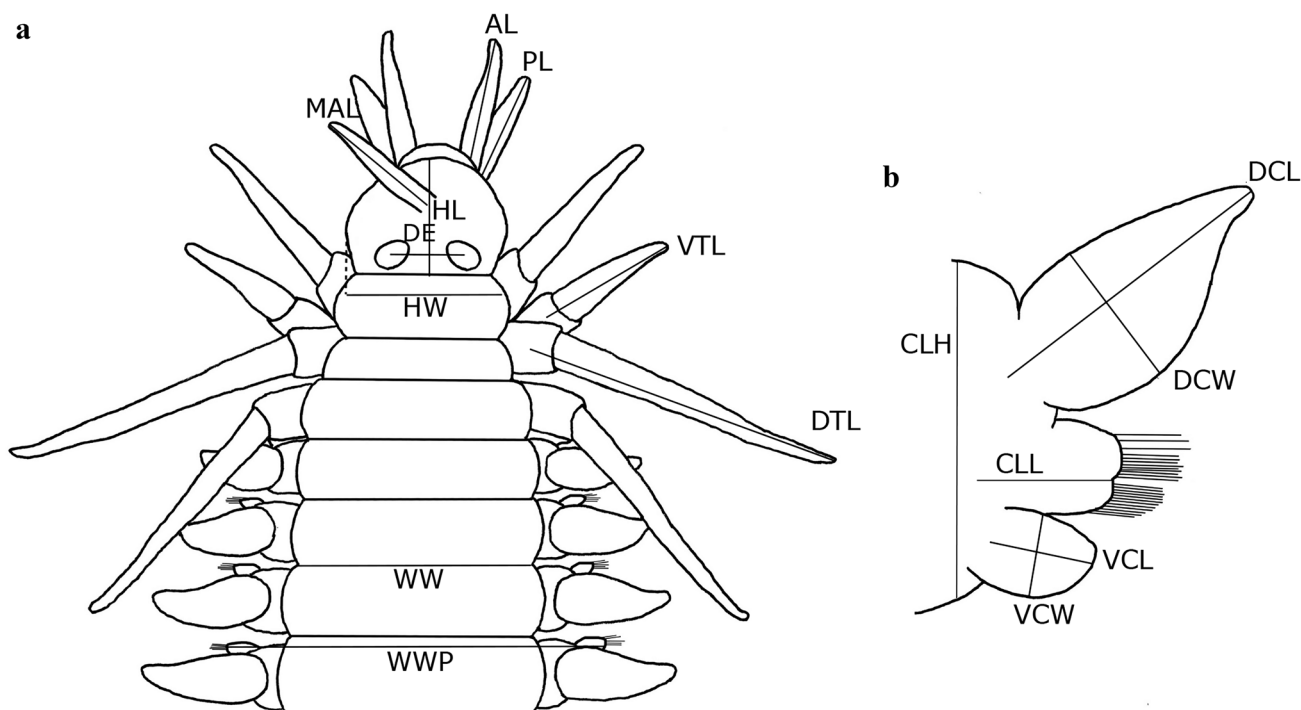
The mean genetic distances (K2P) within and between molecular operational taxonomic units (MOTUs) were calculated in MEGA 10.0.05 using the same GBlock alignment as indicated for nuclear loci.

MOTU clustering

To depict MOTUs, we delineated by applying three delineation methods to both the concatenated mitochondrial and nuclear alignments, except for mtCOI-5P, where we also applied the Barcode Index Number (BIN) implemented in BOLD (Ratnasingham & Hebert, 2013). The Automatic Barcode Gap Discovery (ABGD, Puillandre et al., 2012) was implemented online with default settings using the K2P distance matrix (https://bioinfo.mnhn.fr/abi/public/abgd/abgdweb.html). The Generalized Mixed Yule Coalescent (GYMC) single threshold model (Fujisawa & Barraclough, 2013) and the Poisson Tree Processes (bPTP, Zhang et al., 2013) were implemented online (https://species.h-its.org/). The Bayesian ultrametric tree for the GYMC was generated with BEAST 2.4.6 (Bouckaert et al., 2014) with the appropriate best model (based on AIC criteria; GTR equal rates), and four independent runs for 5—10^7 Markov Chain Monte Carlo (MCMC) generations, sampled every 5,000 generations. The Tracer 1.6 software was used to estimate ESS convergence > 200 for all parameters. The consensus tree was obtained using TreeAnnotator 2.4.6 (Bouckaert et al., 2014) and loaded into Figtree. ML phylogenies contributed for the bPTP results. A final consensus MOTUs was chosen using the majority rule (i.e., most common number of MOTUs).

Genetic diversity and structure

Haplotype networks were made through the PopART software (Leigh & Bryant, 2015). The Templeton, Crandall, and Sing method (TCS, Clement et al., 2002) was used to evaluate the

Fig. 2 Scheme of the morphotype of *Eulalia clavigera*, showing the morphometric measurements used for analysis. **a** Anterior end. **b** Parapodia. Abbreviations: CLL, length of chaetigerous lobes; CLH, height of chaetigerous lobes; AL, length of antennae; PL, length of palps; MAL, length of middle antenna; DTL, length of dorsal tentacular cirri on segment 2; VTL, length of ventral tentacular cirri on segment 2; DCL, length of dorsal cirri; VCL, length of ventral cirri; HL, length of head; WWP, width of worm with parapodia; WW, width of worm without parapodia; HW, width of head; DCW, width of dorsal cirri; VCW, width of ventral cirri; DE, distance between the eyes

relationship between haplotypes and their geographical distribution. GBlocks was not applied in this analysis to avoid underestimating the number of nuclear haplotypes. Indices of genetic diversity (number of haplotypes, h; haplotype diversity, hd; polymorphic sites, S; nucleotide diversity, Pi; Fu & Li D and Tajima D statistical tests) were estimated based on mtCOI-5P for each MOTU using DNASP 5.10 (Librado & Rozas, 2009).

Morphometric analysis

Specimens from four lineages of *Eulalia* were morphometrically compared against each other to complement the molecular data. The remaining lineages had less than three available specimens with a very small size, being therefore unsuitable for morphometric studies and thus have not been named. A minimum of five specimens per population with optimal conditions having all the selected morphological characters and whenever possible, similar in size, were chosen.

The following characters were selected and measured (Fig. 2, supplementary Table S2): the number of segments; the length (mm) of the worm from the prostomium to the pygidium, chaetigerous lobes, terminal antennae, palps, middle antenna, dorsal and ventral tentacular cirrus from the second segment, dorsal and ventral cirri from

median segments, and head; the width (mm) of the worm with and without parapodia (to the tip of the chaetigerous lobes, excluding chaetae) from median segments, head and dorsal and ventral cirri from median segments; and distance between eyes and height (mm) of the chaetigerous lobes. The distance between eyes was measured from the center of the eyespots to avoid possible fixation biases, following Martin et al. (2017). Measurements were done with a LEICA MC170 HD stereo microscope, with an incorporated measurement software. Photographs of live specimens were taken with a Canon EOS1100D camera.

To minimize bias based on size variability, measurements taken to analyze the inter-lineage differences were compared as proportions to create scatter plots between relevant morphological characters and evaluate relationships between the measurements, similar to previous studies (Ravara et al., 2010; Teixeira et al., 2020, 2022). The significance of the inter-population differences using ratios of proportion data (e.g., dividing the length of dorsal cirri against the length of ventral cirri) was also explored by one-way analysis of similarity (ANOSIM), with normalized data based on Euclidean distance resemblance matrices, using PRIMER (2008, version 6.1.11, Plymouth, UK). All remaining analyses were conducted using Microsoft Excel (Office 365 ProPlus).

Fig. 3 Phylogenetic tree and respective COI haplotypes and MOTU locations. **a** Phylogenetic tree reconstructed using Bayesian inference based on concatenated COI, ITS regions and 28S sequences, with information regarding the different MOTU delineation methods. BINs were used only for COI. MOTU GB1 only have COI sequences and was not present in BOLD systems preventing BIN analysis. Only the bootstrap support over 0.85 BI and 85 ML is shown. Each different consensus MOTU is represented by the respective number, with the different colors corresponding to the respective geographic distribution. Live photo belong to the specimen DBUA0002474.02.v01, measuring around 45 mm in length (WL) and exhibiting greenish color. **b** Haplotype network based on COI for all the analyzed MOTUs and outgroups (OUTG). Each haplotype is represented by a circle and number of haplotypes are according to the displayed scale. Numbers correspond to the number of mutational steps between haplotypes. Lines without numbers means only one mutation between haplotypes

Results

Phylogenetic reconstruction

Without any variation in the different delineation methods, nine MOTUs are retrieved from the concatenated Bayesian phylogenetic tree (Fig. 3a), belonging to monophyletic clades with low intraspecific variation (<3%): the previously described *E. clavigera s.s.* (MOTU 4) and *E. viridis* (MOTU 7), six undescribed lineages of *Eulalia*, and the MOTU GB1 from Langeneck et al. (2019). Besides MOTU 4, major clade A englobes four additional MOTUs genetically close to *E. clavigera s.s.* with high bootstrap support: MOTU 1 (unique to the western Mediterranean), MOTU 2 (unique to the subtidal habitats from Madeira), MOTU 3 (the unnamed *Eulalia* KRO53, from the Eastern Mediterranean Sea), and lastly, MOTU GB1 (the Mediterranean *Eulalia cf. clavigera*).

MOTUs 5 and 6 (major clade B) are sister to each other and fall outside the main "*clavigera*" clade. MOTU 5 is present in the British Isles and the Western Mediterranean. The subtidal MOTU 6, together with MOTUs 3 and 8, also subtidal, includes few and very small specimens in relatively poor conditions or exhausted in the DNA analysis and has not been named or used in the morphometric analysis. *Eulalia aurea* was revealed as an actual ingroup for the *E. clavigera/viridis* species complex.

Genetic distances

The global mean genetic distances (K2P) for the *Eulalia* complex and outgroups is detailed in Table 3. Apart from the outgroups and *Eulalia* IT2-1 (MOTU 8), the mean intraspecific distances are 0.93% (0.0–3.3%), with an average congeneric distance of 17.9% (7.1–25.5%) for mtCOI-5P; 1.4% (0.0–3.9%) and 17.2% (4.4–32.6%), respectively, for the ITS region intra- and inter-specific divergence; and 0.04% (0–0.4%) and 2.7% (0–5.9%) for the 28S intra- and inter-specific divergence, respectively. The populations of *E. clavigera s.s.* from continental Europe, and Azores and the Canary islands (MOTU 4) show mtCOI-5P maximum distances up to 3.3% and no considerable divergence (<1%) in the nuclear markers. *Eulalia* IT2-1 has a particularly high inter-specific distance in the nuclear markers, reaching more than 60% for the ITS region and 12% for the 28S locus, similar to those in the *Phyllodoce* sp. (outgroup).

Haplotype networks

Only the 28S network (Fig. 4b) fail to discriminate all the identified MOTUs from the concatenated dataset. It is characterized by a star-shape phylogeny, with most of the unique haplotypes closely related to the common central haplotype, which is composed by MOTUs 1, 3, and 4. However, MOTU 1 also has a distinct haplotype from the common central one, with a similar number of mutations apart, as the outgroup *E. aurea.*
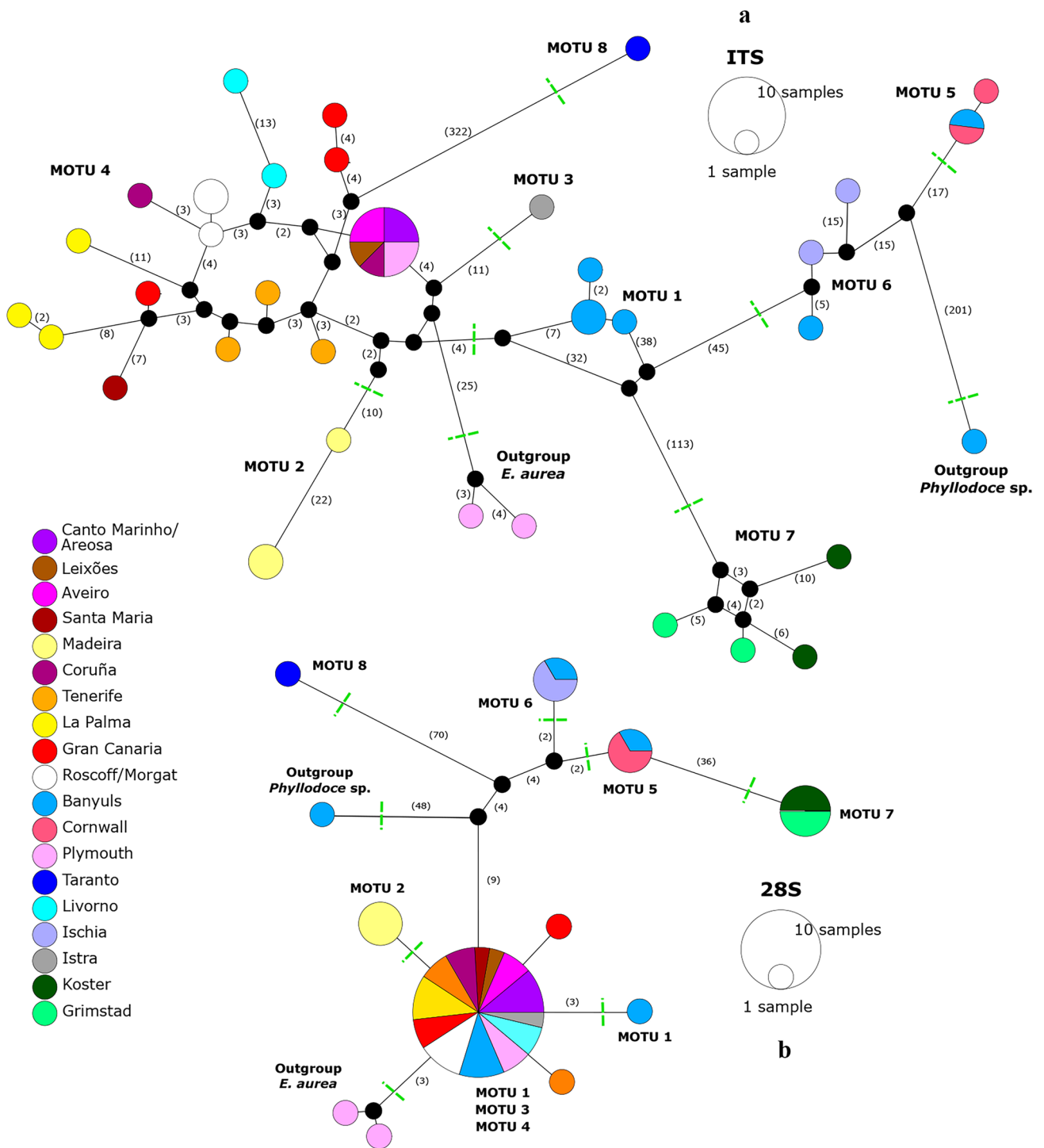
The mtCOI-5P (Fig. 3b) and ITS (Fig. 4a) networks reveal geographically structured populations within MOTU 4, between continental Europe, and Azores and the Canary islands, corresponding to two distinct clades in the BI tree. However, they do not have diverged enough to be divided into two separate MOTUs. Correlations of certain COI haplotypes or parts of the haplotype network with a specific biogeographic region can be found in Madeira (MOTU 2), Scandinavia (MOTU 7), Eastern Mediterranean (MOTU 3), and South of France (MOTU 1).

The mtCOI-5P haplotype diversity is relatively high (Hd > 0.89 to 0.985, Table 4) or even extreme, with almost all specimens having an unique haplotype as in MOTUs 1 (8 haplotypes in 10 specimens) and 2 (11 in 12). None of the MOTUs have a significant Tajima D and Fu and Li's D tests, with the neutral model of nucleotide substitutions being accepted for all the lineages.

Morphometric measurements

The analyses of the most significative morphometric proportions show the formation of independent clusters among the analyzed species (Figs. 5a-h), except for the often-overlapping MOTU 5 and MOTU 4 (*E. clavigera s. s.*). However, despite *E. clavigera s. s.* being considerably larger (both in number of segments and body length and width), MOTU 5 shows similar measurements for dorsal and ventral cirri, head, dorsal tentacular cirri on segment 2, and antennae (Fig. 5a, g). This was further highlighted in Table 5, where very significant proportion ratios (ANOSIM R values close to 1 with p value less than 5%) between these two species were found, in particular, for the length of the dorsal cirri of median segments vs. body width and length (Fig. 5e, f). Global ANOSIM tests for the proportion ratios used in Fig. 5 were also considerably high and the different ratio values are summarized in Table 6 for all the analyzed lineages. The continental Europe and Canarian populations of *E. clavigera s.s.* (MOTU 4) do not differ considerably, except for the larger worm length and number of segments for the latter (Fig. 5f and Table 6). MOTUs 1 and 2 can be mainly distinguished from *E. clavigera s. s.* based on the comparisons between antennae length vs. palp length, length of dorsal tentacular cirri on segment 2 vs. worm width, and distance between eyes vs. head length (Table 6). MOTU 2 shows smaller proportions than the remaining MOTUs, while MOTU 1 mainly appears in an intermediate position. Moreover, besides geographic distribution and live coloration, the length between the chaetigerous lobe vs. ventral cirri seem to be the most significative ratio distinguishing

Fig. 4 Haplotypes networks based on ITS (**a**) and 28S (**b**) for all MOTUs and outgroups, except MOTU GB1. Each haplotype is represented by a circle and number of haplotypes are according to the displayed scale. Colors indicate the geographic location of the haplotype. Numbers correspond to the number of mutational steps between haplotypes. Lines without numbers means only one mutation between haplotypes

Table 3 Mean intra (in bold) and inter-MOTU genetic distances (K2P) for mtCOI-5P, ITS, and 28S, in the nine retrieved MOTUs of *Eulalia* and two outgroups

		Loci	1	2	3	4	5	6	7	8	9	10	11
E. clavigera s.s	1	COI	**1.4 ± 0.3**										
		ITS	**1.7 ± 0.2**										
		28S	**0.0 ± 0.0**										
Eulalia KRO53	2	COI	7.5 ± 1.1	NA									
		ITS	4.8 ± 0.5	NA									
		28S	0.0 ± 0.0	NA									
E. madeirensis sp. nov	3	COI	11.4 ± 1.3	11.8 ± 1.2	**0.8 ± 0.2**								
		ITS	4.6 ± 0.5	6.9 ± 0.7	**0.1 ± 0.1**								
		28S	0.2 ± 0.1	0.1 ± 0.1	**0.0 ± 0.0**								
E. feliciae sp. nov	4	COI	13.9 ± 1.5	14.4 ± 1.6	14.2 ± 1.6	**1.0 ± 0.2**							
		ITS	5.4 ± 0.6	7.6 ± 0.7	7.0 ± 0.7	**2.1 ± 0.4**							
		28S	0.1 ± 0.1	0.1 ± 0.1	0.2 ± 0.1	**0.2 ± 0.1**							
E. viridis	5	COI	23.3 ± 1.9	23.3 ± 1.9	22.0 ± 1.7	21.2 ± 1.8	**0.8 ± 0.2**						
		ITS	29.3 ± 1.8	30.5 ± 1.8	30.8 ± 1.8	28.7 ± 1.7	**2.7 ± 0.4**						
		28S	5.6 ± 0.9	5.6 ± 0.9	5.7 ± 0.9	5.7 ± 0.9	**0.0 ± 0.0**						
E. xanthomucosa sp. nov	6	COI	20.1 ± 1.8	20.1 ± 1.8	19.9 ± 1.6	20.4 ± 1.9	20.3 ± 1.9	**1.3 ± 0.3**					
		ITS	17.3 ± 1.3	18.6 ± 1.4	18.3 ± 1.4	16.4 ± 1.3	27.8 ± 1.8	**0.3 ± 0.1**					
		28S	2.7 ± 0.6	2.7 ± 0.6	2.9 ± 0.6	2.8 ± 0.6	5.1 ± 0.9	**0.0 ± 0.0**					
Eulalia IS-BA	7	COI	18.3 ± 1.6	19.7 ± 1.7	19.9 ± 1.7	19.6 ± 1.8	23.7 ± 2.1	12.1 ± 1.5	**0.3 ± 0.2**				
		ITS	17.7 ± 1.3	19.3 ± 1.4	18.9 ± 1.4	16.2 ± 1.2	27.5 ± 1.3	7.6 ± 0.9	**0.8 ± 0.2**				
		28S	2.7 ± 0.6	2.7 ± 0.6	2.9 ± 0.6	2.8 ± 0.6	5.7 ± 0.9	0.5 ± 0.3	**0.0 ± 0.0**				
E. aurea (OUTG)	8	COI	17.7 ± 1.6	18.4 ± 1.6	19.7 ± 1.8	17.9 ± 1.5	21.4 ± 1.9	15.4 ± 1.6	17.5 ± 1.5	**1.4 ± 0.3**			
		ITS	11.4 ± 1.0	11.8 ± 1.1	13.0 ± 1.1	11.2 ± 0.9	29.1 ± 1.9	17.3 ± 1.7	19.4 ± 1.4	**1.7 ± 0.3**			
		28S	0.6 ± 0.2	0.5 ± 0.2	0.7 ± 0.3	0.6 ± 0.2	5.6 ± 0.9	3.3 ± 0.6	3.0 ± 0.6	**0.3 ± 0.2**			
Eulalia IT2-1	9	COI	24.1 ± 2.0	23.9 ± 2.1	23.4 ± 1.9	24.2 ± 1.9	23.7 ± 2.0	21.8 ± 1.9	24.0 ± 1.9	22.3 ± 1.9	NA		
		ITS	63.9 ± 3.4	65.1 ± 3.5	62.5 ± 3.3	61.8 ± 3.4	59.0 ± 3.3	55.8 ± 3.3	55.5 ± 3.3	62.4 ± 3.5	NA		
		28S	12.5 ± 1.4	12.5 ± 1.4	12.6 ± 1.4	12.5 ± 1.4	14.1 ± 1.5	11.5 ± 1.3	11.5 ± 1.3	12.1 ± 1.3	NA		
Eulalia cf. *clavigera*. (GB1)	10	COI	15.9 ± 1.5	16.3 ± 1.3	16.9 ± 1.6	17.0 ± 1.6	21.6 ± 1.8	19.8 ± 1.7	17.9 ± 1.7	16.8 ± 1.6	21.5 ± 2.0	**0.5 ± 0.2**	
Phyllodoce sp. (OUTG)	11	COI	19.3 ± 1.6	21.3 ± 1.8	21.6 ± 1.8	22.6 ± 1.8	23.2 ± 1.8	18.1 ± 1.6	16.7 ± 1.6	22.2 ± 1.8	24.6 ± 1.9	20.9 ± 1.9	NA
		ITS	48.6 ± 2.5	50.2 ± 2.6	47.9 ± 2.5	48.3 ± 2.5	48.6 ± 2.9	42.2 ± 2.4	43.5 ± 2.4	50.2 ± 2.6	54.9 ± 3.0	NA	NA
		28S	8.1 ± 1.1	8.1 ± 1.1	8.2 ± 1.1	8.2 ± 1.1	9.0 ± 1.2	8.4 ± 1.2	8.4 ± 1.1	8.7 ± 1.1	12.8 ± 1.4	NA	NA

Table 4 Indices of genetic diversity estimated for each species of *Eulalia* and outgroups (OUTG), based on COI. Number of sequences (*n*), nucleotide diversity (*π*), number of haplotypes (*h*), haplotype diversity (Hd), and number of variables sites (*S*). Region abbreviations as in Table 1

	Region	*N*	*h*	Hd	*S*	*π*	Fu and Li's *D*	Tajima's *D*
E. clavigera s. s	PTA; PTN; PTC; SPC; FRR; FRM; GBP; ITL; AM; SI; LP;TE; GC	63	34	0.970	46	0.01326	-1,64,660 *P* > 0.10	-0,48,425 *P* > 0.10
Eulalia KRO53	CI	1	1	-	-	-	-	-
E. madeirensis sp. nov	MP; MF	12	11	0.985	22	0.00838	-1.58386 *P* > 0.10	-1.22113 *P* > 0.10
E. feliciae sp. nov	FRBA	10	8	0.956	18	0.00957	0.01523 *P* > 0.10	-0.24985 *P* > 0.10
E. viridis	SK. NOG; NOE; NOB; NOT; NOF	14	8	0.890	23	0.00802	-1.45830 *P* > 0.10	-1.27765 *P* > 0.10
E. xanthomucosa sp. nov	FRBA; GBC; FRC	11	9	0.964	22	0.01139	-0.13958 *P* > 0.10	-0.17886 *P* > 0.10
Eulalia IS-BA	FRBA; ITI	3	3	1	3	0.00318	-	-
E. aurea	GBP	3	3	1	13	0.01378	-	-
Eulalia IT2-1	ITT	1	1	-	-	-	-	-
Eulalia cf. *clavigera* (GB1)	ITC; ITS	4	4	1	5	0.00486	-0.20080 *P* > 0.10	-0.21249 *P* > 0.10
Phyllodoce sp.	FRBA	1	1	-	-	-	-	-

MOTUs 1 and 2 (Table 5), with MOTU 2 having longer chaetigerous lobes and smaller ventral cirri.

Taxonomic account

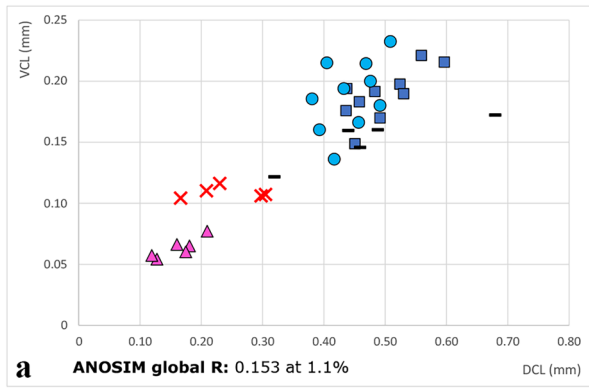### *Eulalia clavigera/viridis* **species complex**.

Diagnosis

Body anteriorly stout and posteriorly tapered, variable in size (length, width, and number of segments). Living specimens may be yellow, but usually green including the pharynx, varying in intensity; once preserved, the pigment fades off into a greenish hue and turning to brownish when aging. Darker, glandular spots usually present laterally from prostomium, in dorsal cirri, along posterior segmental margins but missing in mid-dorsal regions and basally in parapodia. Prostomium rounded triangular, wider than long. Eyes medium-large, rounded, occasionally partly covered by segment 1. Distance between eyes (from center of eyespots) either shorter or as long as head length. Median antenna well in front of eyes, as long as apical ones. Palps as long or slightly longer than antennae. Proboscis widest distally, densely covered with rounded to conical papillae. Terminal ring with varying number of papillae. Longest tentacular cirri may be shorter or slightly longer than body width from median segments. Tentacular cirri of segment 1 reaching about segments 3–5, half as long as dorsal tentacular cirri of segment 2. Dorsal tentacular cirri of segment 2 reaching about segments 6-9, almost two times as long as ventral tentacular cirri (reaching about segments 3-6, often thick and slightly flattened). Dorsal tentacular cirri of segment 3 reaching about segments 6-9, as long as dorsal tentacular cirri of segment 2. Dorsal cirri of median segments asymmetrically lanceolate, about twice as long than wide. Dorsal cirri 2-3 times longer than ventral cirri in median segments. Ventral cirri rounded longer than wide, either smaller or slightly longer than chaetigerous lobes in median segments. Chaetae usually from segment 3, occasionally 1-2 chaetae arising from anterior side of ventral cirrophores of segment 2. Rostrum of chaetal shaft with one large tooth and numerous smaller ones either side, decreasing in size proximally. Blades short. Two pygidial cirri about three times as long as wide, with pointed tips. Median pygidial papilla absent.

Remarks

The description of four, from the eight European lineages belonging to the *E. clavigera/viridis* complex, is provided below, namely, for *E. clavigera s.s.*, *E. feliciae* sp. nov., *E. madeirensis* sp. nov., and *E. xanthomucosa* sp. nov. *Eulalia viridis*, found both in intertidal and subtidal habitats is also part of the complex, as described in Pleijel (1993). The undescribed intertidal *Eulalia* cf. *clavigera* (MOTU GB1), first detected in Langeneck et al. (2019), belongs to the complex, as well as the two remaining rarer and unnamed subtidal lineages from the current study (*Eulalia* KRO53 and *Eulalia* IS-BA).

Besides *E. clavigera s.s.* which is widespread in the North East Atlantic, Azores, Webbnesia, and Western Mediterranean, the remaining lineages seem to be locally restricted. Intertidal specimens from the Azores and Canary

a **ANOSIM global R:** 0.153 at 1.1%

b **ANOSIM global R:** 0.212 at 0.3%

c **ANOSIM global R:** 0.397 at 0.1%

d **ANOSIM global R:** 0.477 at 0.1%

e **ANOSIM global R:** 0.549 at 0.1%

f **ANOSIM global R:** 0.639 at 0.1%

g **ANOSIM global R:** 0.708 at 0.1%

h **ANOSIM global R:** 0.301 at 0.1%

■ *E. clavigera* - Continent ● *E. clavigera* - Islands ▲ *E. madeirensis* sp. nov. ✕ *E. feliciae* sp. nov. — *E. xanthomucosa* sp. nov.

MOTU 4   MOTU 2   MOTU 1   MOTU 5

◄**Fig. 5** Scatter plots with the most considerable proportions in distinguishing *E. clavigera s.s.* (populations from mainland Europe and Canary Islands), *E. feliciae* sp. nov., *E. madeirensis* sp. nov., and *E. xanthomucosa* sp. nov. Significance of the proportion ratios by analysis of similarity (ANOSIM) between all the lineages (Global R) is also indicated. **a** Morphometric proportions between the length of the ventral cirri (VCL) and the length of the dorsal cirri (DCL). **b** Between the length of the head (HL) and the length of the antennae (AL). **c** Between the length of the chaetigerous lobe (CLL) and the length of the ventral cirri (VCL). **d** Between the length of the head (HL) and the width of the head (HW). **e** Between the width of the worm from median segment (WW) and length of the dorsal cirri (DCL). **f** Between the length of the worm (WL) and the length of the dorsal cirri (DCL). **g** Between the width of the worm (WW) and length of the dorsal tentacular cirrus on segment 2 (DTL). **h** Between the lenght of the head (HL) and the distance between the eyes (DE)

archipelagos and North East Atlantic are somewhat similar regarding size, color pattern, and morphological features. Specimens belonging to the "*clavigera*" clade (clade A, Fig. 3a) from the Mediterranean or the subtidal habitats of Madeira (Portugal) are often smaller, may present a yellowish-green (apart from the usual bright or emerald green) live color, more pointed dorsal cirri, and slightly more elongate prostomium. Kato et al. (2001) compiled several *Eulalia* species having green pigmentation, but the only one having uniform pigmentation was *E. viridis*. The latter study apparently overlooked the re-description *of E. viridis* from Bonse et al. (1996), which reinstated *E. clavigera*. Schimmenti et al. (2016) added additional data by summarizing the main morphological differences, including coloration, between *E. ornata*, *E. viridis*, and *E. clavigera s. s.*

The original description highlighted changes in coloration after fixation, where the overall color of *Phyllodoce clavigera*, now *Eulalia clavigera*, is reported as bright green but, through the action of ethanol, changes to metallic brown (Audouin and Milne-Edwards, 1833). Langeneck et al. (2019) indicated a homogeneous coloration in their specimens, but living animals are paler ventrolaterally. Moreover, the pharynx distal papillae change their shape depending on the sample treatment and non-relaxed specimens have globose, low papillae whereas osmotic shocked specimens have them thin, better defined.

Key to the five European *Eulalia* species analyzed in this study:

1. Live specimens with bright yellow coloration; length of the dorsal cirri more than three times longer than ventral cirri of median segments ... *E. xanthomucosa* sp. nov.

— Live specimens with greenish coloration; length of the dorsal cirri less than three times longer than ventral cirri of median segments 2

2(1). Ventral cirri of median segments slightly longer or as long as chaetigerous lobe; relatively large eyes; unique to the Scandinavian region .... *E. viridis*

— Ventral cirri of median segments clearly shorter than chaetigerous lobe; medium-sized eyes; absent in Scandinavian region 3

3(2). Palps as long as antennae; dorsal tentacular cirri on segment 2 clearly shorter than body width of median segments .... *E. clavigera s. s.*

— Palps slightly longer than antennae; dorsal tentacular cirri on segment 2 as long or slightly longer than body width of median segments 4

4(3). Small-sized worm; clearly longer chaetigerous lobes than ventral cirri (1.5x); subtidal and unique to Madeira Island (Portugal) .... *E. madeirensis* sp. nov.

— Small to medium-sized worm; chaetigerous lobes as long or slightly longer than ventral cirri (1.2x); usually intertidal and unique to the Western Mediterranean ... *E. feliciae* sp. nov.

Eulalia clavigera (Audouin & Milne Edwards, 1833) ***s.s.*** (Fig. 1; Fig. 3a).
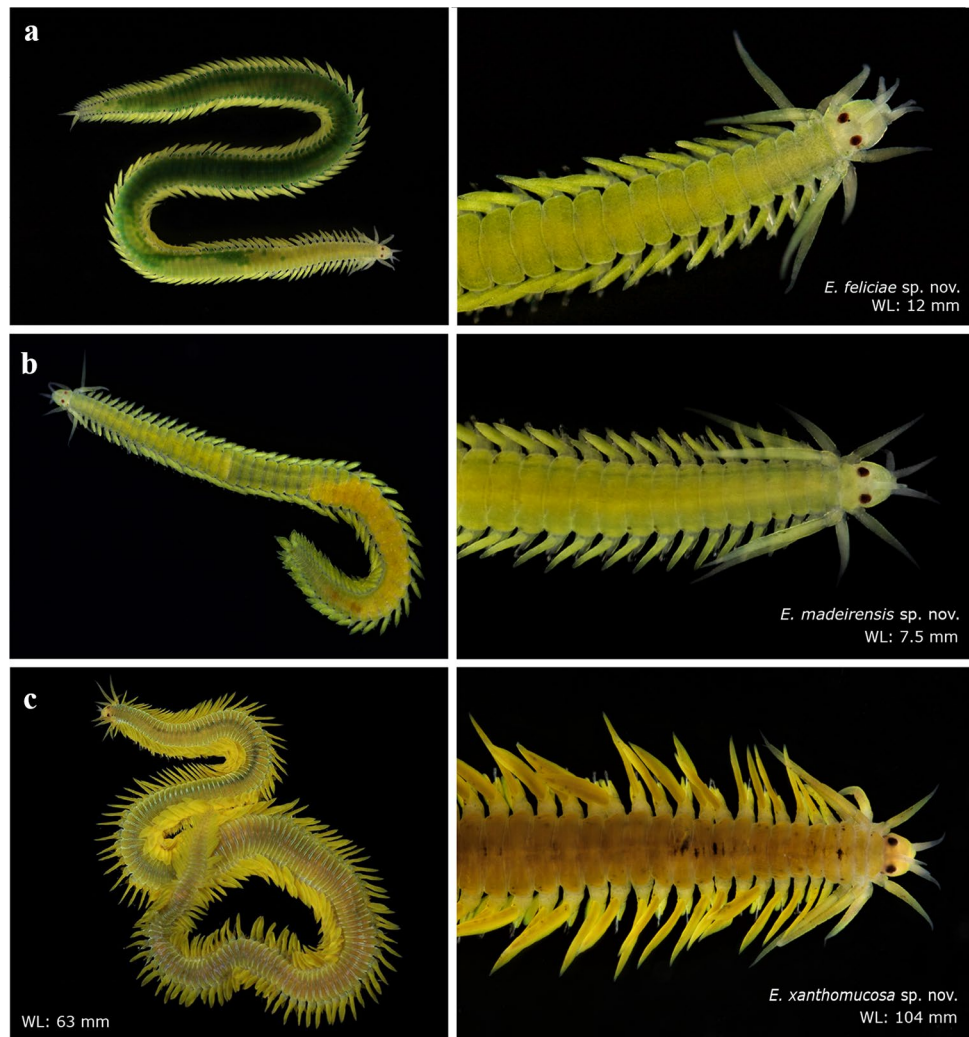*Phyllodoce clavigera* Audouin and Milne-Edwards 1833: 226–228, PL. XVI, Fig. 9–13.
Eulalia clavigera: Bonse et al., 1996: 40–45, Fig. 14 (redescr., syn.); Alós, 2004: 193–196, Fig. 69 (SEM photographs).
? *Eulalia viridis*: Morgado and Amaral, 1983: 51 (non Linnaeus, 1767).

Material examined

Portugal: Aveiro, 6 spms, DBUA0002468.01.v01-v06, 40° 33′ 32.4″ N–8° 46′ 19.2″ W, low tide, among rocks with algae and mussels, collected by Marcos A. L. Teixeira and Ascensão Ravara, 27/07/2018; **Canto Marinho**, 7 spms, DBUA0002469.02.v01-v07, 41° 44′ 13.2″ N–8° 52′ 33.6″ W, low tide, among rocks with algae and mussels, collected by Marcos A. L. Teixeira, 20/05-/2019; **Areosa**, 3 spms, DBUA0002469.01.v01-v03, 41° 42′ 36.0″ N–8° 52′ 12.0″ W, low tide, among rocks with algae and mussels, collected by Marcos A. L. Teixeira, 20/03/2018; **Leixões**, 1 spm, DBUA0002470.01. v01, 41° 10′ 58.8″ N–8° 42′ 18.0″ W, marina in pontoon scrapings, collected by Sofia Duarte, 23/06/2020; **Nazaré**, 3 spms, DBUA0002493.01.v01-v03, 39° 36′ 13.0″ N–9° 04′ 44.0″ W, low tide, among rocks with algae, mussels, barnacles, and *Sabellaria* tubes, collected by Ascensão Ravara, 26/07/2021; **Santa**

Fig. 6 Live, relaxed specimens of *Eulalia* (WL: worm length). **a** *Eulalia feliciae* sp. nov., specimen DBUA0002478.01.v07, dorsal view, greenish coloration. **b** *Eulalia madeirensis* sp. nov., specimen DBUA0002479.01. v03, dorsal view, faint yellowish/light green coloration. **c** *Eulalia xanthomucosa* sp. nov., specimen from the Natural History Museum, London (left) and specimen BI-2014/15–077 (right), dorsal view, bright yellow coloration

E. feliciae sp. nov.
WL: 12 mm

E. madeirensis sp. nov.
WL: 7.5 mm

WL: 63 mm

E. xanthomucosa sp. nov.
WL: 104 mm

Maria (Azores), 2 spm, DBUA0002477.01.v01-v02, 36° 57′ 03.6″ N–25° 01′ 04.8″ W, low tide, among rocks with algae and mussels, collected by Ana Costa, 07/05/2019; **Savage islands**, 1 spm, MB29-000,385, 30° 08′ 23.9″ N–15° 51′ 57.6″ W, low tide, among rocks with algae, kindly provided by the National Museum of Science and Natural History (MUHNAC, Portugal), collected in 22/06/2010. **Spain: Ferrol lagoon (La Coruña)**, 5 spms, DBUA0002473.01.v01-v05, 43° 30′ 07.2″ N–8° 09′ 32.4″ W, low tide, among rocks with algae and mussels, collected by Julio Parapar, 03/02/2015; **Tenerife (Canary islands)**, 11 spms, DBUA0002476.01.v01-v11, 28° 34′ 15.6″ N–16° 20′ 02.4″ W, low tide, among rocks with algae, collected by Marcos A. L. Teixeira, Pedro E. Vieira, José Carlos Hernández, and Beatriz Alfonso, 05/04/2019; **La Palma (Canary islands)**, 10 spms, DBUA0002476.02.v01-v10, 28° 48′ 18.0″ N–17° 45′ 43.2″ W, low tide, among rocks with algae, collected by Marcos A. L. Teixeira and Pedro E. Vieira, 09/04/2019; **Gran Canaria (Canary islands)**, 5 spms, DBUA0002476.03.v01-v05, 27° 59′ 06.0″ N–15° 22′ 33.6″ W, low tide, among rocks with algae, collected by Marcos A. L. Teixeira and Pedro E. Vieira, 06/04/2019.

France: Roscoff, 8 spm, DBUA0002471.01.v01-v08, 48° 43′ 33.6″ N–3° 58′ 40.8″ W, low tide, among rocks with algae and mussels, collected by Arne Nygren, 20/03/2018; **Morgat,** 2 spms, DBUA0002472.01.v01-v02, low tide, among rocks with algae, 48° 13′ 20.3″ N–4° 29′ 42.5″ W, collected by Nicolas Lavesque, 16/06/2018. **Great Britain: Plymouth**, 12 spms, DBUA0002474.01.v01-v05, DBUA0002474.02.v01-v05 and DBUA0002474.03. v01-v02, 50° 21′ 25.2″ N–4° 07′ 40.8″ W, low tide, among rocks with algae and mussels, collected by Arne Nygren and Fredrik Pleijel, 18/03/2006. **Italy: Livorno**, 3 spms, DBUA0002475.01.v01-v03, 43° 32′ 24.0″ N–10° 18′ 00.0″ E, marina in pontoon scrapings, collected by Joachim Langeneck, 20/09/2019.

Measurements

Medium to large-sized worms. Complete specimens up to 275 segments, 68 mm total length and 2 mm maximum width if parapodia included (smallest specimens: 30 mm long, 1.6 mm wide, and 155 segments).

Diagnosis

Living specimens deep green, fading to a greenish hue when preserved and turning to brownish when aging. Prostomium rounded triangular, 1.7 times wider than long. Eyes medium-sized, rounded, occasionally partly covered by segment 1. Distance between eyes (from center of eyespots) either shorter than or as long as head length. Palps as long as antennae. Proboscis widest distally, densely covered with rounded to conical papillae. Terminal ring with varying number of papillae. Longest tentacular cirri clearly shorter than body width from median segments. Tentacular cirri of segment 1 reaching about segment 3, half as long as dorsal tentacular cirri of segment 2. Dorsal tentacular cirri of segment 2 reaching about segment 7, usually 1.9 times as long as ventral tentacular cirri (reaching about segment 3-4, often thick and slightly flattened). Dorsal tentacular cirri of segment 3 reaching about segment 7, as long as dorsal cirri of segment 2. Dorsal cirri of median segments asymmetrically lanceolate, about twice as long than wider. Dorsal cirri 2.5 times longer than ventral cirri in median segments. Ventral cirri rounded 1.5 times longer than wide; twice as short as chaetigorous lobes.

Molecular data

ITS, 28S, and mtCOI-5P sequences as in specimens DBUA0002468.01.v01-v05, DBUA0002469.01.v01-v03, DBUA0002469.02.v01-v05, DBUA0002470.01.v01, DBUA0002471.01. v01-v05, DBUA0002472.01.v01-v02, DBUA0002473.01.v01-v05, DBUA0002474.01.v01-v05, DBUA0002474.02.v01-v05, DBUA0002474.03.v01-v02, DBUA0002475.01.v01-v03, DBUA000 2476.01.v01-v05, DBUA0002476.02.v01-v07, DBUA0002476.03.v01-v05, DBUA0002477.01.v01-v02, and MB29-000385 (Table S1). *Eulalia clavigera s. s.* clearly differs from the remaining species of the complex, grouping in MOTU 4 (Fig. 3a). Interspecific mtCOI-5P mean distances to the closest and distant neighbor are 7.5% (K2P, *Eulalia* KRO53) and 23.3% (K2P, *E. viridis*), respectively. DOI for the species' Barcode Index Number (BIN): https://doi.org/10.5883/BOLD:AAY5110.

Distribution and habitat

North East Atlantic Ocean (United Kingdom, France, Iberian Peninsula) to the Western Mediterranean (Western Italy) and the Canaries, Azores, and Savage archipelagos; introduced in the South-western Atlantic Ocean (Langeneck et al., 2019). Type locality: Brittany, France.

Usually present in intertidal rocky areas with algae, mussels, and barnacles, in association with reefs of *Sabellaria* and in marinas among the algae attached to pontoons.

Reproduction

The available data most likely belong to different lineages (i.e., Scandinavian *E. viridis,* and English and French *E. clavigera*). It has planktonic larvae and reproduces once a year (Meyer, 1938), but the Northern European populations differ in reproduction time, with reproductive cycle starting 4-6 weeks earlier in Swedish than in English and French specimens (Olive, 1975; Pleijel, 1993).

Remarks

Eulalia clavigera was synonymized with *E. viridis* by McIntosh (1908) and later reinstalled by Bonse et al. (1996). These two species slightly differ in prostomial, parapodial, and pharynx papillation features, although the length-to-width ratio of dorsal cirri is the most distinguishing character (Bonse et al., 1996). *Eulalia viridis* has smaller papillae and slender dorsal cirri than *E. clavigera*, the former being restricted to Scandinavian and Northern Sea coasts and seeming to be an intertidal or subtidal northern boreal and sub-arctic species. Conversely, *E. clavigera* is a temperate species, mostly found in intertidal rocky beaches, occurring from Great Britain to the Western Mediterranean Sea, but also in the Azores, Savage, and Canary Islands. Besides the feeding on mussels and barnacles reported in previous studies (Rodrigo et al., 2015), the intertidal Canarian specimens were observed preying on other smaller polychaetes as well.

Phyllodoce gervillei from Granville (France) was erected by Audouin and Milne Edwards (1833), stating that it was identical to *P. clavigera*, except for lacking median antenna and having smaller tentacular cirri. It was also synonymized under *E. viridis* by McIntosh (1908), who considered the absence of antennae as accidental. However, the type locality of *P. gervillei* led us to assume it is most probably a synonym of *E. clavigera*.

Specimens from the type locality of *E. clavigera* (Brittany, France) were collected for this study and grouped in MOTU 4 (Fig. 3a). Only the number of segments and worm length allowed partial separation of the continental European from Canarian populations (Fig. 5f, Table 6). Similarly, despite grouping in two distinct clades and having unique mtCOI-5P and ITS haplotypes, they only diverge up to 3.3% (mtCOI-5P, K2P) and cluster in the same MOTU. *Eulalia clavigera s. s.* usually shows larger proportions in most diagnostic characters than those of the other three species of the complex here described (Fig. 5a-h), especially the longer chaetigerous lobe vs. smaller ventral cirri, the head length/width ratio, and much larger body width vs. smaller dorsal tentacular cirri of segment 2, opposed to the inverse ratio seen in the remaining species of the complex (Table 6). Only *E. xanthomucosa* sp. nov. can often

Table 5 Inter-population differences based on proportion ratios used in the scatter plots of Fig. 5 by analysis of similarity (ANOSIM R significance)

Morphometric proportions	Species/population comparisons	Significance test (ANOSIM)	Morphometric proportions	Species/population comparisons	Significance test (ANOSIM)
DCL/VCL	E. clavigera (continent) vs E. clavigera (islands)	0.145 at 5.9%	HL/AL	E. clavigera (continent) vs E. clavigera (islands)	0.06 at 16.8%
	E. clavigera (continent) vs E. feliciae sp. nov.	0.406 at 1.6%		E. clavigera (continent) vs E. feliciae sp. nov.	0.183 at 9.7%
	E. clavigera (continent) vs E. madeirensis sp. nov.	−0.006 at 44.4%		E. clavigera (continent) vs E. madeirensis sp. nov.	0.209 at 4.8%
	E. clavigera (continent) vs E. xanthomucosa sp. nov.	0.196 at 7.9%		E. clavigera (continent) vs E. xanthomucosa sp. nov.	−0.145 at 87.4%
	E. clavigera (islands) vs E. feliciae sp. nov.	0.114 at 13.4 %		E. clavigera (islands) vs E. feliciae sp. nov.	0.637 at 0.1%
	E. clavigera (islands) vs E. madeirensis sp. nov.	−0.049 at 61.8%		E. clavigera (islands) vs E. madeirensis sp. nov.	0.643 at 0.3%
	E. clavigera (islands) vs E. xanthomucosa sp. nov.	0.355 at 1.6%		E. clavigera (islands) vs E. xanthomucosa sp. nov.	−0.011 at 46.2%
	E. feliciae sp. nov. vs E. madeirensis sp. nov.	0.111 at 19.7%		E. feliciae sp. nov. vs E. madeirensis sp. nov.	−0.173 at 99.6%
	E. feliciae sp. nov. vs E. xanthomucosa sp. nov.	0.22 at 11.1%		E. feliciae sp. nov. vs E. xanthomucosa sp. nov.	0.476 at 2.4%
	E. madeirensis sp. nov. vs E. xanthomucosa sp. nov.	0.099 at 16.2%		E. madeirensis sp. nov. vs E. xanthomucosa sp. nov.	0.455 at 1.1%
VCL/CLL	E. clavigera (continent) vs E. clavigera (islands)	0.005 at 35.4%	HW/HL	E. clavigera (continent) vs E. clavigera (islands)	0.006 at 35.6
	E. clavigera (continent) vs E. feliciae sp. nov.	0.915 at 0.1%		E. clavigera (continent) vs E. feliciae sp. nov.	0.92 at 0.2
	E. clavigera (continent) vs E. madeirensis sp. nov.	0.639 at 0.4%		E. clavigera (continent) vs E. madeirensis sp. nov.	0.795 at 0.2
	E. clavigera (continent) vs E. xanthomucosa sp. nov.	0.212 at 8.3%		E. clavigera (continent) vs E. xanthomucosa sp. nov.	0.994 at 0.2
	E. clavigera (islands) vs E. feliciae sp. nov.	0.854 at 0.1%		E. clavigera (islands) vs E. feliciae sp. nov.	0.403 at 0.8
	E. clavigera (islands) vs E. madeirensis sp. nov.	0.324 at 1.4%		E. clavigera (islands) vs E. madeirensis sp. nov.	0.179 at 6
	E. clavigera (islands) vs E. xanthomucosa sp. nov.	−0.093 at 73.6%		E. clavigera (islands) vs E. xanthomucosa sp. nov.	0.697 at 0.1
	E. feliciae sp. nov. vs E. madeirensis sp. nov.	0.805 at 0.2%		E. feliciae sp. nov. vs E. madeirensis sp. nov.	0.216 at 7.6
	E. feliciae sp. nov. vs E. xanthomucosa sp. nov.	0.886 at 0.8%		E. feliciae sp. nov. vs E. xanthomucosa sp. nov.	0.278 at 6.3
	E. madeirensis sp. nov. vs E. xanthomucosa sp. nov.	0.224 at 5.6%		E. madeirensis sp. nov. vs E. xanthomucosa sp. nov.	0.976 at 0.2
DCL/WW	E. clavigera (continent) vs E. clavigera (islands)	0.053 at 15.2%	DCL/WL	E. clavigera (continent) vs E. clavigera (islands)	0.604 at 0.1%
	E. clavigera (continent) vs E. feliciae sp. nov.	0.369 at 0.6%		E. clavigera (continent) vs E. feliciae sp. nov.	0.468 at 1.2%
	E. clavigera (continent) vs E. madeirensis sp. nov.	0.791 at 0.2%		E. clavigera (continent) vs E. madeirensis sp. nov.	0.967 at 0.1%
	E. clavigera (continent) vs E. xanthomucosa sp. nov.	0.825 at 0.2%		E. clavigera (continent) vs E. xanthomucosa sp. nov.	0.992 at 0.1%
	E. clavigera (islands) vs E. feliciae sp. nov.	0.855 at 0.1%		E. clavigera (islands) vs E. feliciae sp. nov.	0.832 at 0.1%
	E. clavigera (islands) vs E. madeirensis sp. nov.	1 at 0.1%		E. clavigera (islands) vs E. madeirensis sp. nov.	0.967 at 0.1%
	E. clavigera (islands) vs E. xanthomucosa sp. nov.	1 at 0.1%		E. clavigera (islands) vs E. xanthomucosa sp. nov.	0.982 at 0.1%
	E. feliciae sp. nov. vs E. madeirensis sp. nov.	0.272 at 9.3%		E. feliciae sp. nov. vs E. madeirensis sp. nov.	0.203 at 6.1%
	E. feliciae sp. nov. vs E. xanthomucosa sp. nov.	0.276 at 14.3%		E. feliciae sp. nov. vs E. xanthomucosa sp. nov.	0.24 at 4.8%
	E. madeirensis sp. nov. vs E. xanthomucosa sp. nov.	0.091 at 20.3%		E. madeirensis sp. nov. vs E. xanthomucosa sp. nov.	0.101at 19%
DTL/WW	E. clavigera (continent) vs E. clavigera (islands)	0.14 at 64.6%	DE/HL	E. clavigera (continent) vs E. clavigera (islands)	0.034 at 21%
	E. clavigera (continent) vs E. feliciae sp. nov.	0.872 at 0.1%		E. clavigera (continent) vs E. feliciae sp. nov.	1 at 0.2%
	E. clavigera (continent) vs E. madeirensis sp. nov.	0.473 at 0.4%		E. clavigera (continent) vs E. madeirensis sp. nov.	0.99 at 0.1%
	E. clavigera (continent) vs E. xanthomucosa sp. nov.	0.903 at 0.1%		E. clavigera (continent) vs E. xanthomucosa sp. nov.	1 at 0.1%

Table 5 (continued)

Morphometric proportions		Morphometric proportions	
Species/population comparisons	Significance test (ANOSIM)	Species/population comparisons	Significance test (ANOSIM)
E. clavigera (islands) vs E. feliciae sp. nov.	0.111 at 17%	E. clavigera (islands) vs E. feliciae sp. nov.	1 at 0.1%
E. clavigera (islands) vs E. madeirensis sp. nov.	−0.092 at 82.6%	E. clavigera (islands) vs E. madeirensis sp. nov.	0.986 at 0.1%
E. clavigera (islands) vs E. xanthomucosa sp. nov.	0.177 at 8.3%	E. clavigera (islands) vs E. xanthomucosa sp. nov.	1 at 0.2%
E. feliciae sp. nov. vs E. madeirensis sp. nov.	0.23 at 94.3%	E. feliciae sp. nov. vs E. madeirensis sp. nov.	0.104 at 16.5%
E. feliciae sp. nov. vs E. xanthomucosa sp. nov.	0.026 at 44.4%	E. feliciae sp. nov. vs E. xanthomucosa sp. nov.	0.404 at 1.6%
E. madeirensis sp. nov. vs E. xanthomucosa sp. nov.	0.304 at 1.9%	E. madeirensis sp. nov. vs E. xanthomucosa sp. nov.	0.62 at 40.6%

DCL length of dorsal cirri, *VCL* length of ventral cirri, *CLL* length of chaetigerous lobes, *AL* length of antennae, *HL* length of head, *HW* width of head, *WL* worm length, *WW* worm width, *DTL* length of dorsal tentacular cirri on segment 2, *DE* distance between the eyes

share the same morphometric clusters, especially regarding the length of the dorsal cirri, although it tends to show considerably less segments and shorter body length and width than *E. clavigera* s.s.

Eulalia feliciae **sp. nov.**

(Fig. 6a).

Urn:lsid:zoobank.org:act: 9BE4ED06-563E-43C0-9873-D105D88032E4.

Material examined

Type material. **France: Banyuls,** 1 spm, holotype and hologenophore, DBUA0002478.01.v05, 42° 28′ 48.0″ N–3° 08′ 06.0″ E, near shore at 0.5–1 m depth, rocky beach, collected by Arne Nygren and Fredrik Pleijel, 22/04/2001; 5 spms, paratype and paragenophores, DBUA0002478.01.v01-v04 and DBUA0002478.01.v06, 42° 28′ 48.0″ N–3° 08′ 06.0″ E, near shore at 0.5–1 m depth, rocky beach, collected by Arne Nygren and Fredrik Pleijel, 22/04/2001.

Other material. **France: Banyuls**, 2 spms, DBUA0002478.01. v07and MTE040-20, 42° 28′ 48.0″ N–3° 08′ 06.0″ E, near shore at 0.5–1 m depth and subtidal at 10 m depth respectively, among algae, rocks, and mussels, collected by Arne Nygren and Fredrik Pleijel, 02/04/2009; 2 spms, DBUA0002478.01.v08 and MTE042-20, 42° 28′ 48.0″ N–3° 08′ 06.0″ E, subtidal at 10 m depth and near shore at 0.5–1 m depth respectively, among rocks with hydroids, collected by Arne Nygren and Fredrik Pleijel, 05/04/2009.

Measurements

Small to medium-sized worms. Complete specimens up to 135 segments, 14 mm total length and 0.6 mm maximum width if parapodia included (smallest: 9 mm long, 0.5 mm wide, and 93 segments). Holotype lacking posterior end, 14 mm long, 0.6 mm wide, and 135 segments.

Diagnosis

Living specimens deep emerald green (Fig. 6a) fading to a greenish hue once preserved, also when aging. Prostomium rounded triangular, 1.3 times wider than long. Eyes medium-sized, rounded, occasionally partly covered by segment 1. Distance between eyes (from center of eyespots) shorter than head length. Palps slightly longer than antennae. Proboscis widest distally, densely covered with rounded to conical papillae. Longest tentacular cirri slightly longer than body width from median segments. Tentacular cirri of segment 1 reaching segment 3-4, half as long as dorsal tentacular cirri of segment 2. Dorsal tentacular cirri of segment 2 reaching about segment 6-7, usually 1.8 times as long as ventral tentacular cirri (reaching segment 4, often thick

and slightly flattened). Dorsal tentacular cirri of segment 3 reaching about segment 6-7, as long as dorsal tentacular cirri of segment 2. Dorsal cirri of median segments asymmetrically lanceolate, about 2.4 times longer than wide. Dorsal cirri 2.2 times longer than ventral cirri in median segments. Ventral cirri of median segments twice longer than wide; slightly shorter than chaetigerous lobes.

Molecular data

ITS, 28S, and mtCOI-5P sequences as in specimens DBUA0002478.01.v01-v08, MTE040-20, and MTE042-20 (Table S1). *Eulalia feliciae* sp. nov. clearly differs from the remaining species of the complex, grouping in MOTU 1 (Fig. 3a). Inter-specific mtCOI-5P mean distances to the closest and distant neighbor are 13.9% (K2P, *E. clavigera s.s.*) and 22% (K2P, *E. viridis*), respectively. DOI for the species' Barcode Index Number (BIN): https://doi.org/10.5883/DS-MTEFBIN (BIN: BOLD:AEC0502).

Etymology

The new species is named after Felicia Ulltin, a former master student under the supervision of the last author, whose enthusiasm and love for polychaetes are unmatched and an inspiration for future marine researchers.

Distribution

Mediterranean Sea: South of France. Usually present in intertidal or subtidal rocky areas among algae, hydroids and mussels.

Remarks

Besides the molecular data and geographical distribution, *E. feliciae* sp. nov. can be distinguished from *E. clavigera s.s.* and the remaining species from the complex mostly by the deep emerald green coloration in vivo. Moreover, it shows morphometric proportions in most diagnostic characters larger when compared to *E. madeirensis* sp. nov. but smaller against *E. clavigera s. s.* and *E. xanthomucosa* sp. nov. (Fig. 5a-h). The most significant proportions are the ratio between the length of the dorsal vs. ventral cirri, the length of chaetigorous lobe vs. ventral cirri, the length of antennae vs. head, the head length/width, or the distance between eyes vs. head length (Table 6). Moreover, the dorsal tentacular cirri on segment 2 is longer than body width, opposed to the inverse ratio seen in *E. clavigera s.s.*; chaetigerous lobes are only as long or slightly longer than ventral cirri (1.2x), compared to the much larger ratio seen in the other described species; and similar to *E. madeirensis* sp. nov., it shows slightly longer

palps than antennae (Table 6). Furthermore, the dorsal and ventral cirri length ratio is considerably smaller (2.2 times), when compared to *E. xanthomucosa* sp. nov. (3.2 times), *E. madeirensis* sp. nov. (2.6 times), and *E. clavigera s.s* (2.5 times).

Eulalia madeirensis sp. nov.
(Fig. 6b).
Urn:lsid:zoobank.org:act: A107B872-462C-4E36-B15C-5CE02AA71FB7.

Material examined

Type material. **Portugal: Madeira (Funchal),** 1 spm, holotype and hologenophore, DBUA0002479.01.v02, 32° 38′ 09.6″ N–16° 55′ 51.6″ W, subtidal, 11 m depth, collected by Arne Nygren, 21/09/2009; 4 spms, paratypes and paragenophores, DBUA0002479.01.v01, DBUA0002479.01.v03, DBUA0002479.01.v04-v06, 32° 38′ 09.6″ N–16° 55′ 51.6″ W, subtidal, 11 m depth, collected by Arne Nygren, 21/09/2009.

Other material. **Portugal: Madeira (Funchal),** 1 spm, MTE052-20, 32° 38′ 09.6″ N–16° 55′ 51.6″ W, subtidal, 11 m depth, collected by Arne Nygren, 21/09/2009; **Madeira (Porto Moniz),** 4 spms, DBUA0002479.02.v01, MTE053-20, MTE055-20, and MTE057-20, 32° 51′ 38.6″ N–17° 09′ 06.3″ W, subtidal, 11 m depth, collected by Arne Nygren, 30/09/2009.

Measurements

Small-sized worms. Complete specimens up to 115 segments, 10 mm total length, and 0.4 mm maximum width if parapodia included (smallest specimen: 4 mm long, 0.3 mm wide, and 52 segments). Holotype lacking posterior end, 10 mm long, 0.4 mm wide, and 115 segments.

Diagnosis

Living specimens yellowish to light green (Fig. 6b), fading to greenish brown once preserved. Prostomium rounded triangular, 1.4 times wider than long. Eyes medium-sized, rounded, occasionally partly covered by segment 1. Distance between eyes (from center of eyespots) slightly shorter than head length. Palps slightly longer than antennae. Proboscis widest distally, densely covered with rounded to conical papillae. Longest tentacular cirri slightly longer than body width from median segments. Tentacular cirri of segment 1 reaching segment 3-4, as less than half long as dorsal tentacular cirri of segment 2. Dorsal tentacular cirri of segment 2, reaching segment 8, usually 1.7 times longer than ventral tentacular cirri (reaching segment 4-5, being often thick and slightly flattened). Dorsal tentacular cirri of segment 3

reaching about segment 8, as long as dorsal cirri from segment 2. Dorsal cirri of median segments asymmetrically lanceolate, about twice longer than wide. Dorsal cirri 2.6 times longer than ventral cirri in median segments. Ventral cirri of median segments rounded 1.6 times longer than wide; 1.5 times shorter than chaetigorous lobes, much shorter in posterior body half.

Molecular data

ITS, 28S, and mtCOI-5P sequences as in specimens DBUA0002479.01.v01-v06, DBUA0002479.02.v01, MTE052-20- MTE055-20, and MTE057-20 (Table S1). *Eulalia madeirensis* sp. nov. clearly differs from the remaining species of the complex, grouping in MOTU 2 (Fig. 3a). Inter-specific mtCOI-5P mean distances to the closest and distant neighbor are 11.4% (K2P, *E. clavigera s.s.*) and 23.3% (K2P, *E. viridis*), respectively. DOI for the species' Barcode Index Number (BIN): https://doi.org/10.5883/BOLD:AEC0503.

Etymology

The new species is named after Madeira, the main island of the archipelago and the unique remote location where this species can be found so far.

Distribution and habitat

Atlantic Ocean: Exclusive to Madeira Island (Portugal), in subtidal environments up to 11 m depth.

Remarks

Besides the molecular data, bathymetric ranges and geographical distribution, *E. madeirensis* sp. nov. can be distinguished from *E. clavigera s.s.* and the remaining species of the complex mainly by the yellowish light green coloration in vivo, its smaller size and smaller morphometric proportions in most diagnostic characters (Fig. 5h). The most significant ones being the ratio between the length of the dorsal vs. ventral cirri, the length of chaetigorous lobe vs. ventral cirri, the length of antennae vs. head, the head length/width ratio, or the distance between eyes vs. head length (Table 6). Moreover, the dorsal tentacular cirri on segment 2 is longer than body width, opposed to the inverse ratio seen in *E. clavigera s.s.*; chaetigerous lobes are longer than ventral cirri (1.5x); and similar to *E. feliciae* sp. nov., it shows slightly longer palps than antennae (Table 6). Furthermore, the dorsal and ventral cirri length ratio is considerably smaller (2.6 times), when compared to *E. xanthomucosa* sp. nov. (3.2 times).

Further subtidal sampling in other islands from the Azores and Webbnesia is required to see if this species is endemic to Madeira or widespread throughout the different archipelagos.

Eulalia xanthomucosa sp. nov.
(Fig. 6c).
urn:lsid:zoobank.org:act: 70600CFB-9A4D-43D7-9AC5-97BF79FFA046.

Material examined

Type material. **United Kingdom: Cornwall (Newlyn Marina),** 1 spm, holotype and hologenophore, DBUA0002480.01.v07, 50° 06′ 10.8″ N–5° 32′ 49.2″ W, subtidal at 25 m depth, among coralligenous samples, collected by David Fenwick, 02/06/2016; 3 spms, paratypes and paragenophores, DBUA0002480.01.v01-v03, 50° 06′ 10.8″ N–5° 32′ 49.2″ W, lower shore in a rock crevice, collected by David Fenwick, 02/07/2016; 3 spms, paratypes and paragenophores, DBUA0002480.01.v04-v06, 50° 06′ 10.8″ N–5° 32′ 49.2″ W, subtidal at 25 m depth, in rock crevices at *Laminaria* zones and among coralligenous, collected by David Fenwick, 22–08-2017.

Other material. **France: Banyuls,** 1 spm, BI-2014/15–077, 42° 28′ 48.0″ N–3° 08′ 06.0″ E, subtidal at 25 m depth, among algae and boulders, collected by Fredrik Pleijel, 07/04/2009; 1 spm, DBUA0002481.01.v01, 42° 50′ 37.0″ N–3° 14′ 12.0″ E, subtidal at 25 m depth, among coralligenous, collected by Felicia Ulltin, 15/09/2020. **France: Corsica Island,** 2 spms, MNHN-IA-2021–654 and MNHN-IA-2021–655, 41°26'49.2"N–8°54'00.0"E26.8′ N, subtidal at 34 m depth, collected by the CORSICABENTHOS expeditions, 23/10/2020.

Measurements

Medium to large-sized worms. Complete specimens up to 230 segments, 104 mm total length, and 2.378 mm maximum width if parapodia included (smallest specimen: 12 mm long, 0.397 mm wide, and 89 segments). Holotype lacking posterior end, 26 mm long, 1.2 mm wide, and 128 segments.

Diagnosis

Living specimens bright yellow, enhanced by the prevalent yellowish mucus (Figs. 6c and 7a, b), fading to brownish once preserved. Prostomium rounded triangular, 1.1 times wider than long. Eyes medium to largemedium-sized, rounded, occasionally partly covered by segment 1. Distance between eyes (from center of eyespots) clearly shorter than head length. Palps as long as antennae. Proboscis not seen. Longest tentacular cirri slightly longer than body width from median segments. Tentacular cirri of segment 1 reaching segment 4-5, half as long as dorsal tentacular cirri of segment 2. Dorsal tentacular cirri of segment 2 reaching about

Table 6 Summary of the most relevant morphological and morphometric findings rating from 1 (smaller proportions) to 4 (larger proportions) and respective ratio, number of segments (NS), worm length (WL), worm width from median segments (WW), live and preserved coloration, depth and geographical range between the new described species and *E. clavigera s.s*

	E. clavigera s.s.	*E. madeirensis* sp. nov.	*E. feliciae* sp. nov.	*E. xanthomucosa* sp. nov.
DCL/VCL	3 (2.5x)	1 (2.6x)	2 (2.2x)	**3 (3.2x)**
HL/AL	3 (1.7x)	**1 (1.2x)**	**2 (1.2)**	3 (1.6x)
CLL/VCL	4 (2x)	1 (1.5x)	**2 (1.2x)**	3 (1.7x)
HW/HL	**4 (1.7x)**	1 (1.4x)	2 (1.3x)	3 (1.1x)
DCL/WW	**3 (> > WW only)**	1	2	**3**
DCL/WL	**3 (> > WL only)**	1	2	**3**
AL/PL	2 (AL ≈ PL)	**1 (AL < PL)**	2 (**AL < PL**)	2 (AL ≈ PL)
DTL/WW	3 (**DTL < WW**)	1 (DTL > WW)	2 (DTL > WW)	2 (DTL > WW)
DE/ HL	4 (**DE < or ≈ HL**)	1 (DE < HL)	2 (DE < HL)	3 (DE < HL)
NS (mean)	**164 / continent** **221 / islands**	**70**	113	103
WL (mean, mm)	**39.1 / continent** **52.5 / islands**	**6.6**	12.2	16
WW (mean, mm)	**1.3**	**0.209**	0.381	0.551
Color: Live specimens	Green	**Yellowish/light green**	Emerald green	**Bright yellow**
Color: Preserved specimens	Green; Greenish brown; Brown	Greenish brown; Brown	Green; Greenish brown	Brown
Depth (m)	Usually intertidal	**Subtidal (5 - 25)**	Usually Intertidal	**Intertidal, but mostly subtidal (1 - 34)**
Distribution	NE Atlantic; Macaronesia; Western Mediterranean	**Island of Madeira (Portugal)**	**Mediterranean France**	Great Britain; Western Mediterranean

Bold data show considerable differences

DCL length of dorsal cirri, *VCL* length of ventral cirri, *CLL* length of chaetigerous lobes, *PL* length of palps, *HL* length of head, *HW* width of head, *AL* length of antennae, *DTL* length of dorsal tentacular cirri on segment 2, *DE* distance between the eyes

segment 8-9, usually 1.8 times as long as ventral tentacular cirri (reaching segment 5-6, often thick and slightly flattened). Dorsal tentacular cirri of segment 3 reaching about segment 8-9, as long as dorsal cirri from segment 2. Dorsal cirri of median segments asymmetrically lanceolate, about 2.3 times longer than wide. Dorsal cirri 3.2 times longer than ventral cirri in median segments. Ventral cirri of median segments 1.5 times longer than wide; 1.7 times shorter than chaetigerous lobes.

Molecular data

ITS, 28S, and mtCOI-5P sequences as in specimens DBUA0002480.01.v01-v07, DBUA0002481.01.v01, BI-2014/15–077, MNHN-IA-2021–654, and MNHN-IA-2021–655 (Table S1). *Eulalia xanthomucosa* sp. nov. clearly differs from the remaining species of *Eulalia*, grouping in MOTU 5 (Fig. 3a). Inter-specific mtCOI-5P mean distances to the closest and distant neighbor are 12.1% (K2P, *Eulalia* IS-BA) and 20.4% (K2P, *E. feliciae* sp. nov.), respectively. DOI for the species' Barcode Index Number (BIN): https://doi.org/10.5883/BOLD:AEC0501.

Etymology

The new species is named based on its unique bright yellow ("xantho" from ancient Greek) coloration, which is further enhanced by the prevalent and equally yellowish mucus.

Distribution and habitat

Atlantic Ocean: United Kingdom, Cornwall; Mediterranean Sea: France, Banyuls and Corsica Island. Occasional lower intertidal but typically shallow sublittoral in rock crevices at *Laminaria* zones, among coralligenous material in marinas.

Remarks

This species was registered at the Natural History Museum as *Eulalia* sp. "Emits Yellow Mucus A" (tvk NHM-SYS0021180023, https://www.aphotomarine.com/worm_eulalia_species_28-09-11.html). *Eulalia xanthomucosa* sp. nov. differs from *E. clavigera s.s.* and the remaining species from the complex in live coloration (bright yellow instead of

green, with a prevalent presence of yellow mucus; Fig. 7a, b), but may be confused with the also yellowish *E. aurea*. However, it also differs from both *E. aurea* and *E. clavigera s. s.* in having dorsal cirri of median segments much longer in relation to body size (Fig. 5e, f). This feature is more noticeable the larger the specimen is (Fig. 6c). *Eulalia aurea* further differs from *E. xanthomucosa* sp. nov. by the presence of two mid-dorsal red lines (in live specimens only), and two lateral darker lines (Pleijel, 1993). Moreover, the dorsal tentacular cirri on segment 2 is usually longer than body width, opposed to the inverse ratio seen in *E. clavigera s.s.* The latter species has been found living together with *E. xanthomucosa* sp. nov. in Newlyn Marina (Cornwall, United Kingdom), but it usually occurs higher on the shore than *E. xanthomucosa* sp. nov. Marinas are a nurse area for numerous species of epibionts that occur as part of the biofouling community (Hadfield, 2011; Nedved & Hadfield, 2008). Based on our observations, it seems *E. xanthomucosa* sp. nov., a predatory phyllodocid, is recruited to the Newlyn Marina due to the plenty availability of food.

Eulalia xanthomucosa sp. nov. presents larger morphometric proportions in most of the diagnostic characters when compared with *E. feliciae* sp. nov. and *E. madeirensis* sp. nov., (Fig. 5a-h) especially between the length of the dorsal vs. ventral cirri, the length of chaetigerous lobe vs. ventral cirri, the length of antennae vs. head, the head length/width ratio, or the distance between eyes vs. head length (Table 6). However, *E. clavigera s.s.* may have a similar antennae vs. palps ratio and it can often share the same morphometric cluster (Fig. 5a, b, h), but with the analyzed specimens being considerably larger (i.e., longer, wider and with more segments) than the ones from *E. xanthomucosa* sp. nov. Additionally, the eyes are clearly larger for the new species (https://www.aphotomarine.com/images/marine_worms2/worm_eulalia_sp_nov_29-04-22_9.jpg).

Some specimens from *E. xanthomucosa* sp. nov. can also reach similar size as the larger ones belonging to *E. clavigera s.s.* (e.g., DBUA0002481.01.v01: up to 230 segments and 104 mm total length and 2.378 mm maximum width, including parapodia).

Discussion

Recently, a hidden biotechnological potential was uncovered in marine invertebrates, which might offer a wide array of natural products, showing properties compatible with anesthetics, fluorescent probes, and even antibiotics and pesticides (Rodrigo & Costa, 2019). By analyzing the phylogeny of toxin mixtures, Rodrigo et al. (2021a) show that annelids are uniquely positioned in the evolution of animal venoms. In particular, using the toxin-containing mucus present in the green *Eulalia* sp., which based on collection site

(mainland Portugal) corresponds to *E. clavigera s.s.* in our study, revealed possible applications in anti-cancer therapeutics (Rodrigo et al., 2021b) and fluorescent probes for biotechnological applications using a protein mixture from the mucus (Rodrigo, 2020). This highlights the importance of formally describing cryptic complexes, since biochemical features might be unique to each lineage and can have a range of distinct effects and applications.

Molecular tools allowed us to unravel the hidden diversity within *Eulalia*, revealing compelling evidence on the existence of eight European MOTUs within the *E. clavigera* and *E. viridis* pseudo-cryptic complex. Combining molecular, morphometric, coloration, and geographical approaches, we concluded that three of these lineages merit being described as new species. Mean mtCOI-5P distances (17.9%) between lineages fit the annelid species distinction range (Nygren et al., 2018; Ravara et al., 2017; Sampieri et al., 2021), including phyllodocids (e.g. between 22 lineages belonging to the *Eumida sanguinea* (Örsted, 1843) species complex, Teixeira et al., 2022), and the MOTU delineation was congruent among all the methods employed.

We also found a clear geographic structure for most of these European MOTUs. *Eulalia viridis* (MOTU 7) is unique to the Scandinavia and Northern Sea and seems to be a northern boreal and sub-arctic species, occurring both intertidally and sub-tidally waters, in agreement with previous works (Bonse et al., 1996; Kato et al., 2001). *Eulalia clavigera s. s.* (MOTU 4) is a temperate species mostly found in intertidal rocky shores, occurring from Great Britain to the Western Mediterranean, as well as in the Azores, Savage, and Canary archipelagos. Its presence was also confirmed in Argentina (Langeneck et al., 2019). This species seems to be one of the most dominant taxa in Tenerife rocky beaches, including heavily human populated artificial pools in tourist zones, while morphologically similar individuals (lacking molecular data) have been reported from Brazil (Langeneck et al., 2019), with the specimens of *E. viridis* from southern Brazil (Morgado & Amaral, 1983) might actually belong to *E. clavigera* as well.

New continental species

Eulalia clavigera s. s. was considered a Mediterranean relict (Langeneck et al., 2019), while most Mediterranean shallow-water green *Eulalia* probably belong to either one or several different species. At least four different MOTUs seem to be exclusive to the Mediterranean Sea (Fig. 3a, b), a known biodiversity hotspot (Bianchi & Morri, 2000) for cryptic (Calvo et al., 2009; Langeneck et al., 2020; Taboada et al., 2017) and exotic (Galil, 2009; Zenetos et al., 2008) species. The alternating glacial and inter-glacial periods has been often suggested as one of the reasons explaining the high number of Mediterranean species. Under interglacial,

the Mediterranean had a warm and arid climate leading to a deficient water balance, with the entrance of Atlantic surface waters through the Strait of Gibraltar playing a key role. This possibly allowed the introduction and maintenance of (sub) tropical littoral biota (Bianchi et al., 2012), while the North East Atlantic boreal species found refugia in the Mediterranean during glacial periods (Gómez & Lunt., 2007; Maggs et al., 2008; Schmitt et al., 2021). The survival of part of this fauna despite the different environmental (including water temperature) and depth conditions over time sustains the Mediterranean "biodiversity pump" hypothesis, as a possible outcome of the climatic events of the Quaternary (Bianchi & Morri, 2000).

Eulalia feliciae sp. nov. (MOTU 1) seems to be sympatric with *E. clavigera s. s.* (MOTU 4) and *E. xanthomucosa* sp. nov. (MOTU 5) in the Western Mediterranean. Together with a specimen of *E. clavigera s.s.* reported in Langeneck et al. (2019), these three species were collected inter-tidally in Banyuls-sur-Mer. However, as far as we know, *E. xanthomucosa* sp. nov. seems to be more abundant sub-tidally (mainly in recreational marinas), also occurs in Great Britain, and is characteristically yellowish instead of greenish, being thus similar to *E. aurea* coloration-wise. Live coloration is one of the most important taxonomic features in this genus, as most species are similarly brownish when preserved and almost impossible to distinguish based on morphological features (Schimmenti et al., 2016). *Eulalia xanthomucosa* sp. nov. was indeed the most divergent species of the complex and, besides coloration, it differs from *E. clavigera s.s.* morphologically in having longer dorsal and ventral cirri relative to body length and width. These morphological differences appear to parallel the molecular divergence data, e.g., the interspecific nuclear genetic distances tripled (Table 3) compared to those distances found between MOTUs within the major "*clavigera*" clade (clade A, Fig. 3a). The specimens from this clade (with the exception of the population from Madeira) also shared the 28S haplotypes. However, this seems to be common in other closely related marine species (Borges et al., 2012; Vieira et al., 2019). The ancestral central haplotype in the 28S network (Fig. 4b) might suggest the possibility of vicariance-driven speciation through a single colonization event and subsequent diversification (Meißner et al., 2014). The subtidal *Eulalia* IT2-1 (MOTU 8) also has a particularly high inter-specific distance in the nuclear markers, compared to the remaining complex, mirroring the values found for the outgroup (*Phyllodoce* sp.). MOTU 8 belongs to a very small specimen apparently fitting with the morphotype of *E. viridis* (i.e., pointed mid-body dorsal cirri, bright large red eyes). However, it is molecularly highly divergent, showing evidence of an entirely new, yet undescribed species of *Eulalia* outside the *E. clavigera/viridis* species complex.

The unnamed MOTU 3 from Croatia is genetically close to *E. clavigera s.s.* (mtCOI-5P, 7.5%; ITS, 4.8%; no 28S variation), suggesting a recent speciation, unlikely driven by the Messinian salinity crisis (from 6 to 5.33 MY, e.g., Hupało et al., 2019). Instead, this might be explained by environmental driven selection promoting local adaptation (Peijnenburg et al., 2004). The small-size and type locality of MOTU 3 agree with *Eulalia virens* Ehlers, 1864, a junior synonym of *E. viridis* originally described for the Adriatic Sea (Read and Fauchald, 2022). *Eulalia virens* is mainly characterized by its small size (54 segments, 7 mm in length, and 0.5 mm in width), but further sampling is required to allow elucidating if both designations belong or not to the same morphotype/species.

Additional un-sampled European MOTUs of *Eulalia* might still be uncovered. For example, the species *Eulalia (Eumida) microceros* Claparède, 1868, from the Gulf of Naples (synonymized to *E. viridis*) is characterized by its large size (5 cm long, 3 mm wide, and 300 segments). This far surpasses any of the analyzed green specimens of *Eulalia* from continental Europe in this study (Table 6, Table S2), suggesting it might be a large *E. clavigera s.s.* (based on the type locality and original description, PL. XVI, Fig. 4), or another large similar morphotype, different from those we have analyzed. Besides molecular data, morphometry, coloration and geographic restricted locations, reproductive features and gametogenesis could also contribute in future studies to discriminate closely related species, as seen in Sampieri et al. (2020), in which two cryptic *Laeonereis* Hartman, 1945 (family Nereididae) lineages from the West Atlantic coast were distinguished using both mtCOI-5P and histological data.

The Azores and Webbnesia archipelagos

Despite the high incidence of marine invertebrate endemisms in the Azorean ecoregion and Webbnesia (Desiderato et al., 2019; Vieira et al., 2019), no additional intertidal MOTUs were recorded in the Azores and Canary archipelagos. These volcanic islands were never in contact with the continent, were formed at different times, are hundreds of kilometers apart, possess a range of unique geological and climatic conditions, and their biota are the result of dispersal from distant geographical sources and in situ evolution and diversification (Fernández-Palacios et al., 2011). However, their intertidal populations of *Eulalia* do not differ substantially from the continental ones, with the exception of two partial morphometric markers and completely sorted mtCOI-5P and ITS haplotypes (Figs. 3b, 4a, and 5f). Conversely, a new species (*E. madeirensis* sp. nov., MOTU 2) was found in the subtidal populations from Madeira, which agrees with previous findings of cryptic lineages at different depths, e.g.

Fig. 7 Live, relaxed specimens from *E. xanthomucosa* sp. nov. exhibiting yellow coloration and high prevalence of yellowish mucus. **a** Mucus present in the posterior end of the body (specimen from David Fenwick's private collection). **b** Mucus present in the median part of the body (specimen from David Fenwick's private collection)

three MOTUs in *Phyllodoce madeirensis* Langerhans, 1880 (Martin et al., 2021). Additional sampling efforts in Canarian and Azorean subtidal habitats may reveal new species of *Eulalia*. Intertidal populations of *Eulalia* from South Eastern Atlantic (Patagonia, Argentina) also failed to display any molecular or morphological divergence from the European *E. clavigera s. s.* (Langeneck et al., 2019). This may suggest a recent anthropogenically-mediated colonization for both the Canary and the South American populations. Indeed, neither *E. clavigera* nor *E. viridis* were recorded during the intensive surveys done in the 70's, unlike the abundant populations observed recently in Puerto Madryn, Argentina (Orensanz J. M., personal communication in Langeneck et al., 2019). Furthermore, the first records of the *E. clavigera* in Canary date at least from 1976 (Sosa et al., 1976; Núñez et al., 2005; BDBC, https://www.biodiversidadcanarias.es/biota/?lang=en). However, the specimens from the Azores and Canary archipelagos do not share mtCOI-5P or ITS haplotypes with mainland Europe (Figs. 3b and 4a, respectively), suggesting an older non-anthropogenically driven colonization, instead. A recent unintentional introduction of *E. clavigera s. s.* by shipping activities, either with ballast waters or in fouling communities, has been suggested for the Patagonian populations by Schwindt et al. (2014), in a similar way as proved for small benthic marine fishes, chordates, invertebrates, and plankton, introduced either as eggs, larvae, or juveniles, and being first recorded from regions with major commercial ports and heavy international shipping (Cuesta et al., 2016; Lockett & Gomon, 2001; Wonham et al., 2000).

Conclusions

Besides *E. viridis* (restricted to Northern Europe, both in intertidal and subtidal areas) and *E. clavigera s.s.*, we have found six rarer, locally restricted MOTUs within the *Eulalia clavigera/viridis* species complex, with an additional one from the Western Mediterranean reported in a previous study (MOTU GB1). *Eulalia clavigera s. s.* is instead widespread in Europe, being particularly abundant in temperate intertidal areas from the North East Atlantic (ranging from Portugal to the Great Britain), including the Azores and Webbnesia (i.e., Savage and Canary islands), but also with a small presence in the Western Mediterranean, usually in Marina environments. The close genetic proximity but lack of shared haplotypes between the continental and islandic populations of the latter species allows discarding a recent anthropogenic introduction through shipping. Moreover, three new species were described: *Eulalia feliciae* sp. nov., intertidal and unique to the Western Mediterranean, *Eulalia madeirensis* sp. nov., subtidal and unique to the Madeira Island (Portugal), and *Eulalia xanthomucosa* sp. nov., mostly subtidal, with an unique bright yellow coloration within the complex and occurring in the British Isles and southern France. Three unnamed lineages (MOTU GB1, and both the subtidal *Eulalia* KRO53 and *Eulalia* IS-BA) need additional specimens with good structural integrity to attempt a formal description, with the molecular and biogeographical data gathered in this work being a great starting point for future studies.

Declarations

Conflict of interest The authors declare no completing interests.

References

Alós, C. (2004). Familia Phyllodocidae Örsted, 1843. In Vieitez, J. M., Alós, C., Parapar, J., Besteiro, C., Moreira, J., Núñez, J., Laborda, J., & San Martín, G. (Eds.), *Fauna Iberica 25* (pp. 105–209). Madrid: Annelida Polychaeta I. Museo Nacional de Ciencias Naturales. CSIC.

Audouin, J. V., & Milne-Edwards, H. (1833). Classification des Annélides et description de celles qui ornalt les côtes de la France. *Annales des sciences naturelles*, Paris. (series 1), 29, 195–269.

Barfuss, M. H. (2012). Molecular studies in Bromeliaceae: implications of plastid and nuclear DNA markers for phylogeny, biogeography, and character evolution with emphasis on a new classification of Tillandsioideae. Vienna: University of Vienna, 244. Available at: http://othes.univie.ac.at/24037

Bely, A. E., & Wray, G. A. (2004). Molecular phylogeny of naidid worms (Annelida: Clitellata) based on cytochrome oxidase I. *Molecular Phylogenetic and Evolution, 30*(1), 50–63. https://doi.org/10.1016/S1055-7903(03)00180-5

Bianchi, C. N., & Morri, C. (2000). Marine biodiversity of the Mediterranean Sea: Situation, problems and prospects for future research. *Marine Pollution Bulletin, 40*(5), 367–376. https://doi.org/10.1016/S0025-326X(00)00027-8

Bianchi, C. N., Morri, C., Chiantore, M., Montefalcone, M., Parravicini, V., & Rovere, A. (2012). Mediterranean Sea biodiversity between the legacy from the past and a future of change. In N. Stambler (Ed.), *Life in the Mediterranean Sea: A look at habitat changes* (pp. 1–55). Nova Science Publishers Inc.

Bleidorn, C., Kruse, I., Albrecht, S., & Bartolomaeus, T. (2006). Mitochondrial sequence data expose the putative cosmopolitan polychaete *Scoloplos armiger* (Annelida, Orbiniidae) as a species complex. *BMC Evolutionary Biology, 6*(1), 47. https://doi.org/10.1186/1471-2148-6-47

Bonse, S., Schmidt, H., Eibye-Jacobsen, D., & Westheide, W. (1996). *Eulalia viridis* (Polychaeta: Phyllodocidae) is a complex of two species in northern Europe: Results from biochemical and morphological analysis. *Cahiers De Biologie Marine, 37*, 33–48.

Borges, L. M. S., Sivrikaya, H., le Roux, A., Shipway, J. R., Cragg, S. M., & Costa, F. O. (2012). Investigating the taxonomy and systematics of marine wood borers (Bivalvia : Teredinidae) combining evidence from morphology, DNA barcodes and nuclear locus sequences. *Invertebrate Systematics, 26*(6), 572–582. https://doi.org/10.1071/IS12028

Bouckaert, R., Heled, J., Kühnert, D., Vaughan, T., Wu, C. H., Xie, D., Suchard, M. A., Rambaut, A., & Drummond, A. J. (2014). BEAST 2: A software platform for Bayesian evolutionary analysis. *PLOS Computational Biology, 10*(4), e1003537. https://doi.org/10.1371/journal.pcbi.1003537

Calvo, M., Templado, J., Oliverio, M., & Machardom, A. (2009). Hidden Mediterranean biodiversity: Molecular evidence for a cryptic species complex within the reef building vermetid gastropod *Dendropoma petraeum* (Mollusca: Caenogastropoda). *Biological Journal of the Linnean Society, 96*(4), 898–912. https://doi.org/10.1111/j.1095-8312.2008.01167.x

Carr, C. M., Hardy, S. M., Brown, T. M., Macdonald, T. A., & Hebert, P. D. N. (2011). A tri-oceanic perspective: DNA barcoding reveals geographic structure and cryptic diversity in Canadian polychaetes. *PLoS ONE, 6*(7), e22232. https://doi.org/10.1371/journal.pone.0022232

Castresana, J. (2000). Selection of conserved blocks from multiple alignments for their use in phylogenetic analysis. *Molecular Biology and Evolution, 17*(4), 540–552. https://doi.org/10.1093/oxfordjournals.molbev.a026334

Çinar, M. E., & Gönlügür-Demirci, G. (2005). Polychaete assemblages on shallow-water benthic habitats along the Sinop Peninsula (Black Sea, Turkey). *Cahiers De Biologie Marine, 46*, 253–263.

Claparède, É. (1868). Les annélides chétopodes du Golfe de Naples. *Mémoires De La Société De Physique Et D'histoire Naturelle De Genève, 19*(2), 313–584.

Clement, M., Snell, Q., Walke, P., Posada, D., & Crandall, K. (2002). TCS: estimating gene genealogies. In *Proceedings 16th International Parallel and Distributed Processing Symposium* (pp. 7). Presented at the Proceedings 16th International Parallel and Distributed Processing Symposium. IPDPS 2002, Ft. Lauderdale, FL: IEEE. https://doi.org/10.1109/IPDPS.2002.1016585

Cuesta, J. A., Almón, B., Pérez-Dieste, J., Trigo, J. E., & Bañón, R. (2016). Role of ships' hull fouling and tropicalization process on European carcinofauna: New records in Galician waters (NW Spain). *Biological Invasions, 18*(3), 619–630. https://doi.org/10.1007/s10530-015-1034-9

Darriba, D., Taboada, G. L., Doallo, R., & Posada, D. (2012). jModelTest 2: More models, new heuristics and parallel computing. *Nature Methods, 9*(8), 772–772. https://doi.org/10.1038/nmeth.2109

Delić, T., Trontelj, P., Rendoš, M., & Fišer, C. (2017). The importance of naming cryptic species and the conservation of endemic subterranean amphipods. *Scientific Reports, 7*(1), 3391. https://doi.org/10.1038/s41598-017-02938-z

Desiderato, A., Costa, F. O., Serejo, C. S., Abbiati, M., Queiroga, H., & Vieira, P. E. (2019). Macaronesian islands as promoters of diversification in amphipods: The remarkable case of the family Hyalidae (Crustacea, Amphipoda). *Zoologica Scripta, 48*(3), 359–375. https://doi.org/10.1111/zsc.12339

Ehlers, E. H. (1864). Die Borstenwürmer (Annelida Chaetopoda) nach systematischen und anatomischen Untersuchungen dargestellt. Retrieved February 13, 2022, from https://www.biodiversitylibrary.org/page/1985759

Eibye-Jacobsen, D. (1991). A revision of *Eumida* malmgren 1865 polychaeta phyllodocidae. *Steenstrupia*. Retrieved October 25, 2021, from https://eurekamag.com/research/006/964/006964164.php

Eibye-Jacobsen, D. (1993). On the phylogeny of the Phyllodocidae (Polychaeta Annelida): An alternative. *Journal of Zoological Systematics and Evolutionary Research, 31*(3), 174–197. https://doi.org/10.1111/j.1439-0469.1993.tb00188.x

Fernández-Palacios, J. M., de Nascimento, L., Otto, R., Delgado, J. D., García-del-Rey, E., Arévalo, J. R., & Whittaker, R. J. (2011). A reconstruction of Palaeo-Macaronesia, with particular reference to the long-term biogeography of the Atlantic island laurel forests. *Journal of Biogeography, 38*(2), 226–246. https://doi.org/10.1111/j.1365-2699.2010.02427.x

Fernandez-Triana, J. L. (2022). Turbo taxonomy approaches: Lessons from the past and recommendations for the future based on the experience with Braconidae (Hymenoptera) parasitoid wasps. *ZooKeys, 1087*, 199–220. https://doi.org/10.3897/zookeys.1087.76720

Fišer, C., Robinson, C. T., & Malard, F. (2018). Cryptic species as a window into the paradigm shift of the species concept. *Molecular Ecology, 27*(3), 613–635. https://doi.org/10.1111/mec.14486

Folmer, O., Black, M., Hoeh, W., Lutz, R., & Vrijenhoek, R. (1994). DNA primers for amplification of mitochondrial cytochrome c oxidase subunit I from metazoan invertebrates. *Molecular Marine Biology and Biotechnology, 3*, 294–299.

Fujisawa, T., & Barraclough, T. G. (2013). Delimiting species using single-locus data and the Generalized Mixed Yule Coalescent approach: A revised method and evaluation on simulated data sets. *Systematic Biology, 62*(5), 707–724. https://doi.org/10.1093/sysbio/syt033

Galil, B. S. (2009). Taking stock: Inventory of alien species in the Mediterranean Sea. *Biological Invasions, 11*(2), 359–372. https://doi.org/10.1007/s10530-008-9253-y

Grosse, M., Capa, M., & Bakken, T. (2021). Describing the hidden species diversity of *Chaetozone* (Annelida, Cirratulidae) in the Norwegian Sea using morphological and molecular diagnostics. *ZooKeys, 1039*, 139–176. https://doi.org/10.3897/zookeys.1039.61098

Gómez, A., & Lunt, D. H. (2007). Refugia within refugia: Patterns of phylogeographic concordance in the Iberian Peninsula. In S. Weiss & N. Ferrand (Eds.), *Phylogeography of Southern European Refugia* (pp. 155–188). Springer.

Guindon, S., & Gascuel, O. (2003). A simple, fast, and accurate algorithm to estimate large phylogenies by maximum likelihood. *Systematic Biology, 52*(5), 696–704. https://doi.org/10.1080/10635150390235520

Hadfield, M. G. (2011). Biofilms and marine invertebrate larvae: What bacteria produce that larvae use to choose settlement sites. *Annual Review of Marine Science, 3*, 453–470. https://doi.org/10.1146/annurev-marine-120709-142753

Hardy, S. M., Carr, C. M., Hardman, M., Steinke, D., Corstorphine, E., & Mah, C. (2011). Biodiversity and phylogeography of Arctic marine fauna: Insights from molecular tools. *Marine Biodiversity, 41*(1), 195–210. https://doi.org/10.1007/s12526-010-0056-x

Hassouna, N., Mithot, B., & Bachellerie, J. P. (1984). The complete nucleotide sequence of mouse 28S rRNA gene. Implications for the process of size increase of the large subunit rRNA in higher eukaryotes. *Nucleic Acids Research, 12*(8), 3563–3583. https://doi.org/10.1093/nar/12.8.3563

Hupało, K., Teixeira, M. A. L., Rewicz, T., Sezgin, M., Iannilli, V., Karaman, G. S., Grabowski, M., & Costa, F. O. (2019). Persistence of phylogeographic footprints helps to understand cryptic diversity detected in two marine amphipods widespread in the Mediterranean basin. *Molecular Phylogenetics and Evolution, 132*, 53–66. https://doi.org/10.1016/j.ympev.2018.11.013

Hutchings, P., & Kupriyanova, E. (2018). Cosmopolitan polychaetes – fact or fiction? *Personal and Historical Perspectives. Invertebrate Systematics, 32*(1), 1–9. https://doi.org/10.1071/IS17035

Jolly, M. T., Viard, F., Gentil, F., Thiébaut, E., & Jollivet, D. (2006). Comparative phylogeography of two coastal polychaete tubeworms in the Northeast Atlantic supports shared history and vicariant events. *Molecular Ecology, 15*(7), 1841–1855. https://doi.org/10.1111/j.1365-294X.2006.02910.x

Kato, T., Pleijel, F., & Mawatari, S. F. (2001). *Eulalia gemina* (Phyllodocidae: Polychaeta), a new species form Shirahama, Japan. *Proceedings of the Biological Society of Washington, 114*, 381–388.

Katoh, K., & Standley, D. M. (2013). MAFFT multiple sequence alignment software version 7: Improvements in performance and usability. *Molecular Biology and Evolution, 30*(4), 772–780. https://doi.org/10.1093/molbev/mst010

Kumar, S., Stecher, G., Li, M., Knyaz, C., & Tamura, K. (2018). MEGA X: Molecular evolutionary genetics analysis across computing platforms. *Molecular Biology and Evolution, 35*(6), 1547–1549. https://doi.org/10.1093/molbev/msy096

Langeneck, J., Diez, M. E., Nygren, A., Salazar-Vallejo, S., Carrera-Parra, L. F., Vega Fernández, T., Badalamenti, F., Castelli, A., & Musco, L. (2019). Worming its way into Patagonia: An integrative approach reveals the cryptic invasion by *Eulalia clavigera* (Annelida: Phyllodocidae). *Marine Biodiversity, 49*(2), 851–861. https://doi.org/10.1007/s12526-018-0864-y

Langeneck, J., Scarpa, F., Maltagliati, F., Sanna, D., Barbieri, M., Cossu, P., Mikac, B., Galletti, M. C., Castelli, A., & Casu, M. (2020). A complex species complex: The controversial role of

ecology and biogeography in the evolutionary history of *Syllis gracilis* Grube, 1840 (Annelida, Syllidae). *Journal of Zoological Systematics and Evolutionary Research, 58*(1), 66–78. https://doi.org/10.1111/jzs.12336

Leigh, J. W., & Bryant, D. (2015). Popart: Full-feature software for haplotype network construction. *Methods in Ecology and Evolution, 6*(9), 1110–1116. https://doi.org/10.1111/2041-210X.12410

Leite, B. R., Vieira, P. E., Teixeira, M. A. L., Lobo-Arteaga, J., Hollatz, C., Borges, L. M. S., Duarte, S., Troncoso, J. S., & Costa, F. O. (2020). Gap-analysis and annotated reference library for supporting macroinvertebrate metabarcoding in Atlantic Iberia. *Regional Studies in Marine Science, 36*, 101307. https://doi.org/10.1016/j.rsma.2020.101307

Librado, P., & Rozas, J. (2009). DnaSP v5: A software for comprehensive analysis of DNA polymorphism data. *Bioinformatics, 25*(11), 1451–1452. https://doi.org/10.1093/bioinformatics/btp187

Linnaeus, C. V. (1767). Sistema naturae, 12th Edition. Stockholm. pp 1866.

Lobo, L., Ferreira, M. S., Antunes, I. C., Teixeira, M. A. L., Borges, L. M. S., Sousa, R., Gomes, P. A., Costa, M. H., Cunha, M. R., & Costa, F. O. (2017). Contrasting morphological and DNA barcode-suggested species boundaries among shallow-water amphipod fauna from the southern European Atlantic coast. *Genome, 60*(2), 147–157. https://doi.org/10.1139/gen-2016-0009

Lobo, J., Teixeira, M. A. L., Borges, L. M. S., Ferreira, M. S. G., Hollatz, C., Gomes, P. T., Sousa, R., Ravara, A., Costa, M. H., & Costa, F. O. (2016). Starting a DNA barcode reference library for shallow water polychaetes from the southern European Atlantic coast. *Molecular Ecology Resources, 16*(1), 298–313. https://doi.org/10.1111/1755-0998.12441

Lockett, M. M., & Gomon, M. F. (2001). Ship mediated fish invasions in Australia: Two new introductions and a consideration of two previous invasions. *Biological Invasions, 3*(2), 187–192. https://doi.org/10.1023/A:1014584201815

McIntosh, W. C. (1908). A monograph of British Annelids Part I. Polychaeta. Nephthydidae to Syllidae. *Ray Society of London, II., 2*, 1–232.

Maggs, C. A., Castilho, R., Foltz, D., Henzler, C., Jolly, M. T., Kelly, J., Olsen, J., Perez, K. E., Stam, W., Väinölä, R., Viard, F., & Wares, J. (2008). Evaluating signatures of glacial refugia for North Atlantic benthic marine taxa. *Ecology, 89*(11), S108–S122. https://doi.org/10.1890/08-0257.1

Martin, D., Aguado, M. T., Fernández Álamo, M. A., Britayev, T. A., Böggemann, M., Capa, M., Faulwetter, S., Fukuda, M. V., Helm, C., Petti, M. A. V., Ravara, A., & Teixeira, M. A. L. (2021). On the diversity of Phyllodocida (Annelida: Errantia), with a focus on Glyceridae, Goniadidae, Nephtyidae, Polynoidae, Sphaerodoridae, Syllidae, and the Holoplanktonic Families. *Diversity, 13*(3), 131. https://doi.org/10.3390/d13030131

Martin, D., Meca, M. A., Gil, J., Drake, P., & Nygren, A. (2017). Another brick in the wall: Population dynamics of a symbiotic species of *Oxydromus* (Annelida, Hesionidae), described as new based on morphometry. *Contributions to Zoology, 86*(3), 181–211. https://doi.org/10.1163/18759866-08603001

Meißner, K., Bick, A., Guggolz, T., & Götting, M. (2014). Spionidae (Polychaeta: Canalipalpata: Spionida) from seamounts in the NE Atlantic. *Zootaxa, 3786*(3), 201–245. https://doi.org/10.11646/zootaxa.3786.3.1

Meyer, A. (1938). Der Rogen und die Entwicklung der trochophora von *Eulalia viridis*. *Biologia Generalis, 14*, 334–389.

Miglietta, M. P., Faucci, A., & Santini, F. (2011). Speciation in the sea: Overview of the symposium and discussion of future directions. *Integrative and Comparative Biology, 51*(3), 449–455. https://doi.org/10.1093/icb/icr024

Morgado, E. H., & Amaral, A. C. Z. (1983). Anelídeos poliquetos associados ao briozoário *Schizoporella unicornis* (Johnston):

IV. Phyllodocidae e Hesionidae. *Revista Brasileira De Zoologia, 2*, 49–54. https://doi.org/10.1590/S0101-81751983000200002

Morton, B. (2011). Predator–prey-scavenging interactions between *Nucella lapillus*, *Carcinus maenas* and *Eulalia viridis* all exploiting *Mytilus galloprovincialis* on a rocky shore recovering from tributyl-tin (TBT) pollution. *Journal of Natural History, 45*(39–40), 2397–2417. https://doi.org/10.1080/00222933.2011.596637

Nedved, B. T., & Hadfield, M. G. (2008). *Hydroides elegans* (Annelida: Polychaeta): A model for biofouling research. In H. C. Flemming, R. Venkatesan, S. P. Murthy, & K. E. Cooksey (Eds.), *Marine and Industrial Biofouling* (pp. 203–218). Springer.

Núñez, J., Brito, M. C., & Docoito, J. R. (2005). Annelid polychaetes from Canaries: Catalogue of species, distribution and habitats. *Vieraea, 33*, 297–332.

Nygren, A., Eklöf, J., & Pleijel, F. (2009). Arctic-boreal sibling species of *Paranaitis* (Polychaeta, Phyllodocidae). *Marine Biology Research, 5*(4), 315–327. https://doi.org/10.1080/17451000802441301

Nygren, A. (2014). Cryptic polychaete diversity: A review. *Zoologica Scripta, 43*(2), 172–183. https://doi.org/10.1111/zsc.12044

Nygren, A., Eklöf, J., & Pleijel, F. (2010). Cryptic species of *Notophyllum* (Polychaeta: Phyllodocidae) in Scandinavian waters. *Organisms Diversity & Evolution, 10*(3), 193–204. https://doi.org/10.1007/s13127-010-0014-2

Nygren, A., Parapar, J., Pons, J., Meißner, K., Bakken, T., Kongsrud, J. A., Oug, E., Gaeva, D., Sikorski, A., Johansen, R. A., Hutchings, P. A., Lavesque, N., & Capa, M. (2018). A mega-cryptic species complex hidden among one of the most common annelids in the North East Atlantic. *PLoS ONE, 13*(6), e0198356. https://doi.org/10.1371/journal.pone.0198356

Nygren, A., & Pleijel, F. (2011). From one to ten in a single stroke – resolving the European *Eumida sanguinea* (Phyllodocidae, Annelida) species complex. *Molecular Phylogenetics and Evolution, 58*(1), 132–141. https://doi.org/10.1016/j.ympev.2010.10.010

Olive, P. J. W. (1975). A vitellogenesis promoting influence of the prostomium in the polychaete *Eulalia viridis* (müller) (phyllodocidae). *General and Comparative Endocrinology, 26*(2), 266–273. https://doi.org/10.1016/0016-6480(75)90145-8

Peijnenburg, K. T. C. A., Breeuwer, J. A. J., Pierrot-Bults, A. C., & Menken, S. B. J. (2004). Phylogeography of the planktonic Chaetognath *Sagitta setosa* reveals isolation in European Seas. *Evolution, 58*(7), 1472–1487. https://doi.org/10.1111/j.0014-3820.2004.tb01728.x

Pleijel, F. (1993). Polychaeta Phyllodocidae. *Marine Invertebrates of the Scandinavia, 8*, 1–159.

Puillandre, N., Lambert, A., Brouillet, S., & Achaz, G. (2012). ABGD, Automatic Barcode Gap Discovery for primary species delimitation. *Molecular Ecology, 21*(8), 1864–1877. https://doi.org/10.1111/j.1365-294X.2011.05239.x

Rambaut, A., Drummond, A. J., Xie, D., Baele, G., & Suchard, M. A. (2018). Posterior summarization in Bayesian phylogenetics using tracer 1.7. *Systematic Biology, 67*(5), 901–904. https://doi.org/10.1093/sysbio/syy032

Ratnasingham, S., & Hebert, P. D. N. (2013). A DNA-based registry for all animal species: The Barcode Index Number (BIN) system. *PLoS ONE, 8*(7), e66213. https://doi.org/10.1371/journal.pone.0066213

Ravara, A., Cunha, M. R., Pleijel, F. (2010). Nephtyidae (Annelida, Polychaeta) from southern Europe. *Zootaxa, 2682*, 1–68. https://doi.org/10.11646/zootaxa.2682.1.1

Ravara, A., Ramos, D., Teixeira, M. A. L., Costa, F. O., & Cunha, M. R. (2017). Taxonomy, distribution and ecology of the order Phyllodocida (Annelida, Polychaeta) in deep-sea habitats around the Iberian margin. *Deep Sea Research Part II: Topical Studies in Oceanography, 137*, 207–231. https://doi.org/10.1016/j.dsr2.2016.08.008

Springer

GfBS

Read, G., & Fauchald, K. (Ed) (2022). World Polychaeta Database. *Eulalia virens* Ehlers, 1864. Retrieved January 10, 2022, from World Register of Marine Species at: https://www.marinespecies.org/aphia.php?p=taxdetails&id=339528

Rodrigo, A. P., Costa, M. H., de Matos, A. P. A., Carrapiço, F., & Costa, P. M. (2015). A Study on the digestive physiology of a marine polychaete (*Eulalia viridis*) through microanatomical changes of epithelia during the digestive cycle. *Microscopy and Microanalysis, 21*(1), 91–101. https://doi.org/10.1017/S143192761401352X

Rodrigo, A. P., & Costa, P. M. (2019). The hidden biotechnological potential of marine invertebrates: The polychaeta case study. *Environmental Research, 173*, 270–280. https://doi.org/10.1016/j.envres.2019.03.048

Rodrigo A. P. (2020). The biotechnological value of a novel potent marine biotoxin from the polychaete worm *Eulalia viridis*: chemical and toxicological evaluation. Universidade Nova Lisboa. PhD thesis. Retrieved January 10, 2022, from https://hdl.handle.net/10362/116178

Rodrigo, A. P., Grosso, A. R., Baptista, P. V., Fernandes, A. R., & Costa, P. M. (2021a). A transcriptomic approach to the recruitment of venom proteins in a marine annelid. *Toxins, 13*(2), 97. https://doi.org/10.3390/toxins13020097

Rodrigo, A. P., Mendes, V. M., Manadas, B., Grosso, A. R., Alves de Matos, A. P., Baptista, P. V., Costa, P. M., & Fernandes, A. R. (2021b). Specific antiproliferative properties of proteinaceous toxin secretions from the marine annelid *Eulalia* sp. onto ovarian cancer cells. *Marine Drugs*, *19*(1), 31. https://doi.org/10.3390/md19010031

Ronquist, F., & Huelsenbeck, J. P. (2003). MrBayes 3: Bayesian phylogenetic inference under mixed models. *Bioinformatics, 19*(12), 1572–1574. https://doi.org/10.1093/bioinformatics/btg180

Sampieri, B. R., Steiner, T. M., Baroni, P. C., da Silva, C. F., Teixeira, M. A. L., Vieira, P. E., Costa, F. O., & Amaral, A. C. Z. (2020). How oogenesis analysis combined with DNA barcode can help to elucidate taxonomic ambiguities: a polychaete study-based approach. *Biota Neotropica, 20*. https://doi.org/10.1590/1676-0611-BN-2020-0959

Sampieri, B. R., Vieira, P. E., Teixeira, M. A. L., Seixas, V. C., Pagliosa, P. R., Amaral, A. C. Z., & Costa, F. O. (2021). Molecular diversity within the genus *Laeonereis* (Annelida, Nereididae) along the west Atlantic coast: Paving the way for integrative taxonomy. *PeerJ, 9*, e11364. https://doi.org/10.7717/peerj.11364

Schimmenti, E., Musco, L., Brutto, S. L., Mikac, B., Nygren, A., & Badalamenti, F. (2016). A Mediterranean record of *Eulalia ornata* (Annelida: Phyllodocidae) corroborating its fidelity link with the *Sabellaria alveolata*-reef habitat. *Mediterranean Marine Science*, *17*(2), 359–370. https://doi.org/10.12681/mms.1485

Schmitt, T., Fritz, U., Delfino, M., Ulrich, W., & Habel, J. C. (2021). Biogeography of Italy revisited: Genetic lineages confirm major phylogeographic patterns and a pre-Pleistocene origin of its biota. *Frontiers in Zoology, 18*(1), 34. https://doi.org/10.1186/s12983-021-00418-9

Schwindt, E., Gappa, J. L., Raffo, M. P., Tatián, M., Bortolus, A., Orensanz, J. M., Alonso, G., Diez, M. E., Doti, B., Genzano, G., Lagger, C., Lovrich, G., Piriz, M. L., Mendeza, M. M., Savoya, V., & Sueiro, M. C. (2014). Marine fouling invasions in ports of Patagonia (Argentina) with implications for legislation and monitoring programs. *Marine Environmental Research, 99*, 60–68. https://doi.org/10.1016/j.marenvres.2014.06.006

Sosa, A., Núñez, J., & Bacallado, J.J. (1976). Contribución al estudio de los poliquetosen Canarias. I: Aphroditidae, Amphinomidae, Phyllocidae y Eunicidae. *Vieraea*, 6(2), 231–252

Taboada, S., Leiva, C., Bas, M., Schult, N., & McHugh, D. (2017). Cryptic species and colonization processes in *Ophryotrocha* (Annelida, Dorvilleidae) inhabiting vertebrate remains in the shallow-water Mediterranean. *Zoologica Scripta, 46*(5), 611–624. https://doi.org/10.1111/zsc.12239

Teixeira, M. A. L., Vieira, P. E., Pleijel, F., Sampieri, B. R., Ravara, A., Costa, F. O., & Nygren, A. (2020). Molecular and morphometric analyses identify new lineages within a large *Eumida* (Annelida) species complex. *Zoologica Scripta, 49*(2), 222–235. https://doi.org/10.1111/zsc.12397

Teixeira, M. A. L., Vieira, P. E., Ravara, A., Costa, F. O., & Nygren, A. (2022). From 13 to 22 in a second stroke: Revisiting the European *Eumida sanguinea* (Phyllodocidae: Annelida) species complex. *Zoological Journal of the Linnean Society, 196*(1), 169–197.

Ushakov, P. L. (1972). Polychaetes of the sub-order Phyllodociforma of the Polar Basin and the North Western part of the Pacific. In Russian. Translated by the Israel Program for Scientific Translations: Jerusalem, 1974. *Fauna SSSR, 102*, 1–271.

Vieira, P. E., Desiderato, A., Holdich, D. M., Soares, P., Creer, S., Carvalho, G. R., Costa, F. O., & Queiroga, H. (2019). Deep segregation in the open ocean: Macaronesia as an evolutionary hotspot for low dispersal marine invertebrates. *Molecular Ecology, 28*(7), 1784–1800. https://doi.org/10.1111/mec.15052

Viéitez, J. M., Alós, C., Parapar, J., Besteiro, C., Moreira, J., Núñez, J., Laborda, A. J. & San Martín, G. (2004). Annelida Polychaeta I. In Ramos, M. A. et al. (Eds). Fauna Ibérica, Vol. 25 (530 pp). *Museo Nacional de Ciencias Naturales CSIC*. Madrid

Wonham, M. J., Carlton, J. T., Ruiz, G. M., & Smith, L. D. (2000). Fish and ships: Relating dispersal frequency to success in biological invasions. *Marine Biology, 136*(6), 1111–1121. https://doi.org/10.1007/s002270000303

Zenetos, A., Meric, E., Verlaque, M., Galli, P., Boudouresque, C. F., Giangrande, A., Cinar, M., & Bilecenoglu, M. (2008). Additions to the annotated list of marine alien biota in the Mediterranean with special emphasis on Foraminifera and Parasites. *Mediterranean Marine Science*, *9*(1), 119–166. https://doi.org/10.12681/mms.146

Zhang, J., Kapli, P., Pavlidis, P., & Stamatakis, A. (2013). A general species delimitation method with applications to phylogenetic placements. *Bioinformatics, 29*(22), 2869–2876. https://doi.org/10.1093/bioinformatics/btt499